National Park Service
U.S. Department of the Interior

Science Report NPS/SR—2026/460
https://doi.org/10.36967/2318166

Maritime Influence on Climate Futures at Point Reyes National Seashore and Bodega Bay

Clouds and fog borne off the Pacific regularly frame Drakes Bay at Point Reyes National Seashore.
NPS / DOUGLAS SMITH

Maritime Influence on Climate Futures at Point Reyes National Seashore and Bodega Bay

Science Report NPS/SR—2026/460

Gregory C. Arena [1], Lorraine Parsons [2]

[1] University of California, Davis
Department of Environmental Science and Policy
1 Shields Ave.
Davis, CA 95616

[2] National Park Service
Point Reyes National Seashore
1 Bear Valley Rd.
Point Reyes Station, CA 94956

Please cite this publication as:

Arena, G.C., and L. Parsons. 2026. Maritime Influence on Climate Futures at Point Reyes National Seashore and Bodega Bay. Science Report NPS/SR—2026/460. National Park Service, Fort Collins, Colorado. https://doi.org/10.36967/2318166

NPS 612/199752, July 2026

This report is available in digital format from the National Park Service DataStore and the Natural Resource Publications Management website. If you have difficulty accessing information in this publication, particularly if using assistive technology, please email irma@nps.gov.

Contents

Contents (continued)

Page

Figures

Page

Figures (continued)

Page

Tables

Page

Abstract

Shaped by diverse landscapes and microclimates, the future of the unique ecology of Point Reyes National Seashore is imperiled by climate change. Climate modeling can offer park managers important insights into how these systems may change in a warmer and drier future. But maritime effects such as offshore wind, fog and low clouds are difficult to account for in current park modeling. In this report, we looked at a combined 37 years of data collected between two meteorological stations located at coastal sites at Point Reyes (G Ranch) and neighboring Bodega Bay, to identify trends and to compare against future climate projections. These long-term data sets were consistent with modeled climate change trends regarding both temperature increase and observed increase in 99^{th} percentile heat events. While the future of annual precipitation at Point Reyes remains uncertain, climate models anticipate a long-range increase in water deficit as warmer temperatures drive greater evaporative demand. However, data collected at Bodega Bay instead illustrated a moderate increase in relative humidity (RH) and decline in vapor pressure deficit (VPD) over the past three decades. Regression analysis between measured climate variables at both sites highlighted the important role that summertime low clouds and fog may play in reducing VPD in areas influenced by maritime climate. Low cloud and fog events may serve to offset increases in soil and ambient temperature, as well as temperature extremes. These events may also reduce moisture loss from this system during critical times of the year and buffer extended drought anticipated in some climate models. Fog and cloud coverage may therefore act to limit potential hydraulic and thermal stress experienced by grass and forbs native to the Point Reyes Peninsula. Further data that can directly measure fog and low cloud events and the impact and extent of these patterns on both water and energy balance will be important in assessing maritime influence on climate change across the Seashore.

List of Terms

Climate Futures: A description of the physical attributes of climate that could plausibly occur at a specific place and time in the future. Multiple climate futures are used to consider the range of ways climate could change, using up to 40 models, incorporating known physical parameters and trends.

Climatic Water Deficit: An indicator of landscape aridity by quantifying the deficit of water available to plants, calculated as potential ET minus actual ET.

Diablo Winds: Hot, dry winds with a northeast to east bearing that occur in the northern San Francisco Bay Area that can occur between late fall and early winter.

Energy Balance: The process by which plants maintain thermal equilibrium with their environment by modulating input and output of heat.

Entrainment: The process by which parcels of air homogenize as air mixes via convection.

Evaporative Demand: The potential for water to evaporate from the land surface as determined by physical parameters such as temperature, relative humidity and air flow as well as biological parameters such as stomatal conductance/resistance.

Evapotranspiration (ET): The combined loss of water through evaporation from land surfaces, and transpiration, or the evaporation of water from plant tissues.

Fog and Low Clouds: Fog and low clouds include cloud formations below 6,500 feet. Fog is defined as all clouds forming at sea level. (For this report fog is not distinguished between advective and evaporative fog.) While low clouds may occupy the same altitude as fog, low clouds originate from higher altitudes and are not formed at sea level.

Latent Heat Transfer: Thermal equilibrium driven by the release or absorption of heat via phase change, such as through evaporative cooling from perspiration or transpiration.

Sensible Heat Transfer: Thermal equilibrium driven by the release or absorption of heat sans phase change, such as through conduction and convection where there is contact between two mediums.

Solar Radiation: The energy released from the sun. This includes ultraviolet waves (UV), photosynthetically active radiation (PAR), and near infrared heat (NIR).

Vapor Pressure Deficit (VPD): The difference between the quantity of water held in the atmosphere and the atmosphere’s capacity to hold water.

Water Balance: An accounting of the movement of water through systems (i.e., precipitation, run-off, evaporation). For plants this includes transpiration (affected by stomata and morphology).

Coming to Terms with Climate Change offers a comprehensive list of relevant NPS definitions.

Acknowledgments

Peer reviews of this report by David J. Lawrence (Climate Change Response Program [CCRP], National Park Service [NPS]), Michael Tercek (Science Consultant, Walking Shadow Ecology), and David Press (Point Reyes National Seashore, NPS). Peer review management by Wylie Carr (CCRP, NPS). This report also benefitted from feedback and support provided by Mark Schwartz (Department of Environmental Science and Policy, University of California Davis) as well as Rachel Clemesha and Alexander Gurshunov (Scripps Institution of Oceanography). Publication process managed by the National Park Service Inventory & Monitoring Division Science Report Series publication team, with editorial support provided by Stacie L. Findon and formatting by Alyssa S. McGinnity, Lise Grace, and Fagan Johnson. Special thanks to Gregory McCurdy and Pamela Lacy (Desert Research Institute) and Anna M. Wilson (Scripps Institution of Oceanography) for their assistance with data procurement.

Executive Summary

Point Reyes National Seashore (hereafter Point Reyes, Seashore, or the park) represents an important refugium for native flora and fauna. The diversity of life represented within the park is a testament to equally diverse microclimates, defined by topography and maritime influence. In a warming world, climate models that incorporate physical parameters help conceptualize future scenarios and goals for NPS resource managers. But attributes that define the unique landscape of the Seashore, such as fog, low clouds, wind, and other meteorological factors vary with both altitude and coastal proximity and are difficult to model. To better understand the unique conditions of the Seashore, ambient temperature, relative humidity, precipitation, wind speed, wind direction, soil moisture, soil temperature, and solar radiation were collected from two coastal meteorological stations located at Point Reyes G Ranch and Bodega Marine Laboratory. The combined 37 years of data were interpreted with consideration of climate futures developed for the park by the NPS Climate Change Response Program. To broadly incorporate park natural resource management concerns and the biological significance of report findings, the analysis was also situated within a context of plant water and energy balance.

Two climate futures, characterized as warm-wet and hot-dry, describe a spectrum of relatively drier conditions defined by greater volatility and an increase in 99th percentile heat events and changes in precipitation extremes. Coastal meteorological data at G Ranch and Bodega Bay showed consistency with these modeled warming trends. Historical warming at G Ranch fell between the predicted values for these futures. Data from both sites indicated an increase in 99th percentile heat events. Precipitation data for Bodega Bay and Point Reyes indicated no significant change in total annual precipitation, nor any change in 99th percentile precipitation events. Increasing climate water deficit has been anticipated as a most likely outcome under both warm-wet and hot-dry futures as rising global temperatures increase evaporative demand. However, the Bodega Bay dataset did not align with this projection, illustrating a 37-year increase in RH during the driest months of the year and a corresponding decline in vapor pressure deficit over this period.

The use of solar radiation and RH as indicators of low clouds and fog cover highlights the important role that maritime influence may play in reducing VPD. Low cloud cover and fog appear to offset rises and extremes in both soil and air temperatures, while also helping to reduce moisture loss from these systems. Additionally, the relationship between wind speed and both solar radiation and RH indicated the important role of convection in the formation and dissipation of low cloud, fog, and precipitation in Point Reyes.

Continued monitoring of climate variables will be vital to honing our understanding of the interrelationship and trajectory of climate change at the Seashore. Data collection for fog and low cloud-coverage events and soil surface temperature will be especially pertinent for determining the role of maritime influences in dampening adverse, volatile climate futures. Already, G Ranch and Bodega Bay datasets indicate that maritime conditions may limit the potential for both hydraulic and thermal stress among flora on the Point Reyes Peninsula.

Introduction

Intersecting the San Francisco Bay Area biodiversity hotspot, Point Reyes National Seashore is pivotal to the conservation of unique native life and landscapes. The mosaic of distinct ecosystems incorporated within the Seashore offers critical refuge for many rare and endemic species (Evens 2008; NPS 2025). Located on the western, Pacific edge of Marin County, approximately 30 miles north of San Francisco, the Seashore includes 81 miles of coastline and 1407 feet of elevational gain (NPS 2025). While Point Reyes has been federally protected since 1962, ongoing management is complicated by the uncertainties of global climate change. This report aims to highlight current and future conditions, vulnerabilities and management needs of park resources by analyzing trends in climate variables at Point Reyes and by comparison against future climate projections for the Seashore.

The continued protection of natural and cultural resources relies on stewardship that can prepare for and respond to a range of climate futures in park planning (Alizadeh 2022; CCRP 2024; Winsberg 2012). Over 200 days of fog, strong onshore wind, and proximity to unique features such as the Pacific Ocean, Tomales Bay, and San Francisco Bay define the region's microclimates (García-Reyes and Largier 2012; Ingraham and Matthews 1995; Figure 1). Yet abiotic conditions such as wind and occult precipitation—fog, mist, and low clouds—present uncertainties in the fidelity of climate projections for Point Reyes and the California Coast (CCRP 2024; John et al. 2024; Kulkarni et al. 2019; Steeneveld et al. 2014). The exclusion of these maritime influences can produce biased climate models that misrepresent complex interactions and resource conditions (Iacobellis and Cayan 2013; Clemesha et al. 2017; Pierce et al. 2014). Both water balance—the accounting of the movement of water through a system through precipitation, run-off, evaporation and transpiration—and energy balance—the process of thermal equilibrium with systems—are directly impacted by a warm-wet or hot-dry future (Geiger et al. 1995). How climate change will affect resource conditions is integral to future ecological response and may be conceptualized through water and energy balance as a way to more thoroughly understand the biological significance of these climate trends.

Figure 1. Microclimates of Point Reyes. Left: G Ranch Meteorological Station lies approximately 0.5 miles from Point Reyes North Beach, on the leeward side of the coastal dunes. Right: The footbridge at Home Ranch roughly corresponds to the centroid of the Seashore, the basis of CCRP's climate modeling for the park.

Coastal fog and low cloud cover and wind have a pronounced effect on water balance within systems like Point Reyes (Figure 2). These factors directly influence vegetation growth and distribution patterns (Jones 2013; McCree 1971; Sridhar and Elliott 2002). Temperature and humidity changes driven by fog or low clouds can dramatically alter vapor pressure deficit (VPD), which is defined as the difference between the quantity of water held in the atmosphere and the atmosphere's capacity to hold water (Lambers et al. 1998). As this deficit grows, there is an increased evaporative demand applied to the land surface and plant tissue. This deficit can exacerbate drought-related stress (Grossiord et al. 2020; Schönbeck et al. 2022). Additionally, fog and clouds can introduce water in the form of precipitation and fog deposition (Fischer et al. 2009). Understanding the effects of wind on water balance is also essential to vegetation management. Contact between plant tissue and the external environment informs rates and modes of gas exchange and the loss of moisture from plant and land surfaces through evapotranspiration (Ehleringer and Björkman 1978; Finnigan 2021). Wind is also a vector for introducing cool, wet, hot, or dry air to a site, and along the California Coast, prevailing wind directions have been correlated with fog formation and input (García-Reyes and Largier 2012; Torregrosa et al. 2015).

Figure 2. Point Reyes National Seashore, surrounding features, and points of interest.
NPS / GREGORY ARENA

Both fog and low cloud cover and wind also impact energy balance within plant ecosystems (Jones 2013; McCree 1971; Sridhar and Elliott 2002). Rates of heat loss from plant tissue and land surfaces are governed by the air's capacity to hold heat—defined by relative humidity, air density, and convection (Jones 2013; Gomez et al. 2023). Impacts of wind on evapotranspiration are interconnected with sensible heat loss—passive transfer of heat driven by the interface between biotic or abiotic surfaces and the environment—and latent heat loss—transfer of heat through evaporation (Aylor et al. 1973; Schymanski et al. 2017; Wang et al. 2020). Additionally, fog and cloud coverage play an important role in regulating incoming solar radiation. Clouds and aerosols block or diffuse light such as ultraviolet (UV), photosynthetically active radiation (PAR), and near infrared heat (NIR; Inada 1976). Low clouds can also regulate heat loss by reflecting or re-radiating heat and moderating ambient and surface temperatures.

The variable influences on maritime systems (such as fog, low clouds, and wind) are difficult to integrate within climate models (Pierce et al. 2014). The National Park Service's Climate Change Response Program has developed two climate futures for Point Reyes—warm-wet and hot-dry (CCRP 2024). These futures identify divergent scenarios from 40 climate model outputs and posit two climate futures which offer a range of temperature increase and aridification. While there is consensus within current climate models that Point Reyes is warming, the future of precipitation and water balance remain uncertain (CCRP 2024). Fortunately, National Park Service (NPS) partners, Desert Research Institute and Scripps Institution, have collected continuous meteorological data at coastal sites at Point Reyes and Bodega Bay for a combined 37 years (DRI 2025; UCD, n.d.). Analysis of data collected at these meteorological stations provides an opportunity to better understand past and current changes in climate. These data in turn help interpret climate futures for Point Reyes. Through this report, we explore maritime influence through the specific relationship between wind, cloud coverage, ambient temperatures, relative humidity (RH), soil moisture, soil temperatures and precipitation in the context of water and energy balance at Point Reyes and Bodega Bay to examine how present climate trends may impact natural resources at the Seashore.

Methods

Past climate data were derived from two meteorological stations and included wind speed, wind direction, soil moisture (% volumetric water content) and soil temperature (°C) at 10 cm, ambient temperatures (°C), solar radiation (Watts/m^2), relative humidity (%) and precipitation (inches). For the analysis in this report, °C was converted to °F. In the absence of low cloud and fog data, solar radiation was used as a proxy in this analysis. Solar radiation expresses the total inbound quantity of energy per unit time. This includes UV, PAR and NIR (Inada 1976). Cloud coverage can attenuate wavelengths across these spectrums impacting observed incoming solar radiation in total and at discrete times. Vapor pressure deficit was calculated as the difference between the saturation vapor pressure (P calculated by Tetens's formula) and the actual vapor pressure (derived from RH).

For Temperature (T) in °C Tetens's formula for Saturation Vapor Pressure (P) is given as:

$$P = 0.61078 \exp((17.27T) / (T + 237.3))$$

Vapor Pressure is given as:

$$VPD = P*(1-RH/100)$$

A meteorological station at G Ranch in the Seashore (38°05'39" N, 122°57'03" W) included all of the above climate variables. These data were used to highlight Point Reyes specific trends and for comparison of abiotic variables such as soil temperature and soil moisture, which were specific to this location. The meteorological station has been managed by the DRI (an affiliate of the University of Nevada, Reno) since 2006 with some interruption in 2014 and 2015 due to battery issues (Appendix B). All data sourced from G-Ranch were in intervals of 10 minutes with the exception of precipitation which was in daily intervals.

Precipitation data and long-term temperature and RH data were also sourced from a meteorological station located at the Bodega Marine Laboratory (BML), at Bodega Bay (38°19'12" N, 123°04'04" W). For this analysis, Bodega Bay data, reflecting 1988 to 2025, were used for long-term patterns and to supplement absent data. The Bodega Bay lab and meteorological station are managed by the University of California Davis. Temperature and RH data for BML have been historically used as suitable analogs for the Point Reyes coastline (Ryan and Parsons 2011). All data sourced from BML were in intervals of 1 hour with the exception of precipitation, which was in daily intervals.

Both DRI and BML perform some level of quality control. Where DRI data indicated clear sensor errors these data were removed from analysis. In other instances, data were less obviously a sensor error, such as in the case of unseasonable precipitation events or unusually high temperatures. In these instances, a comparison was made against BML data or NOAA daily regional averages. If the data appeared unreasonable, they were removed from analysis. Where there appears to be sudden breaks in trends we consulted with DRI or BML to identify if these trends were connected to meteorological station maintenance. To account for data excluded from analysis, the following steps were taken: years or relevant months where there was missing data that would impact totals or averages for those years or months were excluded from time-series analysis. For event analysis, event-percentages rather than event-totals were used to reduce biasing.

Based on two-way ANOVA comparisons we found no average statistically significant difference in the shape of seasonal trends for ambient temperature, RH, and solar radiation between these two meteorological stations, all $p > 0.99$. However, throughout the year, Bodega Bay was on average 0.9°F warmer than Point Reyes G Ranch, $F(1,228) = 16.4$, $p < 0.001$, RH was 2.4% lower, $F(1,190) = 25.2$, $p < 0.0001$, and solar radiation was 7 watts m^{-2} lower, $F(1,213) = 6.72$, $p = 0.01$. There was no significant difference in the shape of seasonal precipitation patterns between sites, $p > 0.51$. While Bodega Bay receives a mean 0.45 inches more precipitation per month, this distinction was also insignificant, $p > 0.09$. Unlike RH, ambient temperatures, and solar radiation, between years precipitation is more variable by month along the California Coast (García-Reyes and Largier 2012).

Meteorological data were compared against two divergent climate futures, warm-wet and hot-dry, generated by the NPS Climate Change Response Program (CCRP) and centered on the year 2050. Following the methods of Runyon et al. (2024), these divergent and plausible futures were selected by choosing the extreme ends of climate projections from 40 global climate models (GCMs) under two emission scenarios (RCP 4.5 and 8.5), thus bracketing the full range of climate uncertainty across the projections. More specifically, the warm-wet and hot-dry climate futures for the Seashore came from CNRM-CM5.rcp45 and MIROC-ESM.rcp85 projections, respectively. Approximation of local climate futures to a scale of 1 km^2 requires a process known as downscaling (Hall et al. 2024; Pielke and Wilby 2012). Warm-wet and hot-dry climate futures utilize statistically downscaled gridMET data localized to the park centroid which lies approximately 5.5 km (3.4 miles) from the Pacific Coast (Figure 2). Through the process of downscaling, model outputs incorporate a gridded data set, MACAv2-METDATA (Multivariate Adaptive Constructed Analogs), which improves model fit through comparison with this high-resolution data (McSweeney 2018; Pierce and Cayan 2016). The GCMs, which are foundational to these products, incorporate equations representative of the physical parameters of various abiotic factors—including meteorological means and fluctuations and global patterns such as the circulation of ocean currents and atmospheric cells (GFDL 2025; McSweeney 2018).

Statistical Analysis

Assumption testing was incorporated into all models to test for Type 1 errors. For comparisons among abiotic conditions, linear regression was applied with post-hoc Tukey test. For analysis of data with cyclical patterns such as monotonic trends, we performed a Mann–Kendall test, with plotted amplitudes and Sen's slope estimate. Box-Cox or log transformations were applied to the data to improve normality (identified in relevant figures). Welch's ANOVA with Games–Howell post hoc test was used to assess statistical significance. For analysis where time was not a direct consideration, year, month, day, and hour were incorporated (when relevant) as random effects.

Estimates of change in the number of extreme (99^{th} percentile) precipitation events were plotted for all instances during which more than 2.6 inches of rain occurred within a 24-hour period. (2.6 inches were determined by CCRP as the historical, average 99^{th} percentile for the Seashore). Average precipitation within a 24-hour period per year, was calculated by averaging all days during which there was greater than >0.01 inches of rainfall per 24-hour day. From these yearly averages 99^{th} percentile precipitation events were also separately calculated for each year. For comparison of wind speed against RH, RH was subdivided into bins spanning 10% change in RH and rendered as a box and whisker plot. This was done to improve visualization of the data, highlight potential outliers, and indicate general clustering of RH and wind speeds. To better understand the interplay between abiotic factors at these sites and times of year when both water and energy balance are most acute, much of the analysis is confined to critical months and hours. June through August are both the months with the least precipitation and the greatest fog cover (Ingraham and Matthews 1995). Fog dissipation during the summer months in Point Reyes and Bodega Bay typically occurs in the early afternoon between 12 and 3 pm, standard time, making these timeframes important for analysis of wind on cloud cover and RH (personal observation). Because wind and RH are frequently associated with the convective effects of the sun's rays, analyses were limited to specific times or hours to exclude within-day variations and plotted to strategically correspond with times when wind was anticipated to be at a maximum and/or cloud coverage most likely to dissipate (Appendix A; Geiger et al. 1995).

Wind direction was subdivided into 22.5° segments to determine modal wind and mean direction based on a 16-point compass. Analysis of change in wind direction was based on the dominant wind bearings observed by month. Analysis was also performed on wind direction by month, with respect to bearings associated with Diablo Wind events.

All data and R code are included as supplemental materials upon request through CCRP (contact: climate_change@nps.gov).

Results

Summary tables of all statistical tests performed on data for Bodega Bay (1988–2025) and Point Reyes G Ranch (2006–2025) meteorological stations (Tables 1–5).

Table 1. Summary of relationships between environmental variables and time, meteorological drivers, and site conditions at Bodega Bay and Point Reyes G Ranch. To reduce the impact of random factors (month, day, hours), some comparisons are restricted to specific months such as June, July, and August, or specific times of day. The rationale for these constraints is described in the Methods section. An en dash "–" indicates a non-directional significant relationship (e.g., wind bearing), "***NS"*** indicates no statistical significance, and "***NA***" indicates absence of data for analysis.

	BODEGA BAY		**POINT REYES G RANCH**	
TEST	**TREND**	**STATISTICAL SIGNIFICANCE**	**TREND**	**STATISTICAL SIGNIFICANCE**
air °F (max) vs. time	***NS***	R^2 = 0.01 p = 0.49	**Positive Correlation**	R^2 = 0.71 p = 0.00012 F(1,17) = 41.3
air °F range vs. time	**Positive Correlation**	R^2 = 0.61 p < 0.0001 F(1,34) = 54.1	***NS***	R^2 = 0.18 p = 0.07
air °F vs. RH	**Negative Correlation**	R^2 = 0.06 p < 0.0001 F(1,3942) = 1262.3	**Negative Correlation**	R^2 = 0.81 p < 0.0001 F(1,806301) = 1.4e+6
air °F 99th % vs. time	**Positive Correlation**	T = 0.29 p = 0.0362	**Positive Correlation**	T = 0.48 p = 0.00526
soil °F (max) vs. time	***NA***	–	**Negative Correlation**	R^2 = 0.51 p < 0.0001 F(1,405) = 416
soil °F vs. solar rad [A]	***NA***	–	**Positive Correlation**	R^2 = 0.22 p = 0.01 F(1,1571) = 430.1
soil °F range vs. time	***NA***	–	**Negative Correlation**	R^2 = 0.31 p < 0.0001 F(1,1571) = 701
soil VWC vs. time	***NA***	–	**Positive Correlation**	R^2 = 0.11 p < 0.0001 F(1,2.3e+5) = 2.8e+4
soil VWC vs. soil °F	***NA***	–	**Negative Correlation**	R^2 = 0.55 p < 0.0001 F(1,36822) = 4.5e+4
solar rad vs. time	**Negative Correlation**	R^2 = 0.86 p < 0.00001 F(1,15) = 90.4	**Negative Correlation**	T = −0.09 p = 0.000002
solar rad vs. wind m/s	**Positive Correlation**	R^2 = 0.56 p < 0.0001 F(1,1109) = 134.1	**Positive Correlation**	R^2 = 0.14 p < 0.0001 F(1,2890) = 471
precip. vs. time [B]	***NS***	R^2 = 0.03 p = 0.31	***NS***	R^2 = 0.01 p = 0.19
precip vs. wind °	***NS***	R^2 = 0.02 p = 0.38	**–**	R^2 = 0.37 p = 0.0072 F(1,16) = 9.48

[A] Soil temperature vs. solar radiation: includes months 6–8 and restricted to hours 12–1 pm.

[B] Precip vs. time: analysis of change in precipitation between years for both yearly and monthly totals.

[C] Wind ° vs. time: specific details outlined in Tables 2–4.

Table 1 (continued). Summary of relationships between environmental variables and time, meteorological drivers, and site conditions at Bodega Bay and Point Reyes G Ranch. To reduce the impact of random factors (month, day, hours), some comparisons are restricted to specific months such as June, July, and August, or specific times of day. The rationale for these constraints is described in the Methods section. An en dash "–" indicates a non-directional significant relationship (e.g., wind bearing), "***NS"*** indicates no statistical significance, and "***NA***" indicates absence of data for analysis.

	BODEGA BAY		**POINT REYES G RANCH**	
TEST	**TREND**	**STATISTICAL SIGNIFICANCE**	**TREND**	**STATISTICAL SIGNIFICANCE**
RH vs. time	**Positive Correlation**	$R^2 = 0.19$ $p = 0.01102$ $F(1,31) = 7.31$	***NS***	$R^2 = 0.0$ $p = 0.91$
RH vs. wind m/s	**Negative Correlation**	$R^2 = 0.004$ $p < 0.0001$ $F(1,10982) = 37.77$	**Negative Correlation**	$p = 0.0072$ $F(1,17896) = 99.51$
RH vs. wind °	***NS***	$R^2 = 0.02$ $p = 0.34$	***NS***	$R^2 = 0$ $p = 0.84$
VPD vs. time	**Negative Correlation**	$R^2 = 0.21$ $p = 0.00581$ $F(1,32) = 8.739$	***NS***	$R^2 = 0.04$ $p = 0.40$
VPD vs. RH	**Negative Correlation**	$R^2 = 0.93$ $p < 0.0001$ $F(1,12788) = 168588$	**Negative Correlation**	$R^2 = 0.88$ $p < 0.0001$ $F(1,16) = 127.52$
VPD vs. wind °	**–**	$R^2 = 0.002$ $p < 0.0001$ $F(1,284888) = 475.8$	***NS***	$R^2 = 0.01$ $p = 0.65$
VPD vs. wind m/s	**Positive Correlation**	$R^2 = 0.007$ $p < 0.0001$ $F(1,12788) = 1.7e+5$	**Positive Correlation**	$R^2 = 0.23$ $p = 0.042$ $F(1,16) = 4.86$
wind ° vs. time [C]	**–**	$R^2 = 0.14$ $p = 0.0214$ $F(1,36) = 5.79$	**–**	$R^2 = 0.60$ $p = 0.00002$ $F(1,18) = 21.95$
wind m/s vs. time	***NS***	$R^2 = 0$ $p = 0.35$	**Negative Correlation**	$R^2 = 0.002$ $p < 0.0001$ $F(1,842656) = 1920$

[A] Soil temperature vs. solar radiation: includes months 6–8 and restricted to hours 12–1 pm.

[B] Precip vs. time: analysis of change in precipitation between years for both yearly and monthly totals.

[C] Wind ° vs. time: specific details outlined in Tables 2–4.

Table 2. Primary winds. For both sites, northwest to north (315–360°) were the primary wind directions for most of the year. At Bodega Bay, east-northeast to east-southeast (67.5–112.5°) were the second most frequent wind bearings and predominated in some months. At Point Reyes G Ranch, east to south (90–180°) were the second most frequent wind bearings. “Increase” indicates a rise in the proportion of winds from a given bearing over time; “***NS***” indicates no statistical significance. A statistically significant change in the proportion of winds associated with Diablo wind bearings was observed in only two months.

	BODEGA BAY NW-N 315–360°		**POINT REYES G RANCH NW-N 315–360°**	
SEASON (MONTHS)	**TREND**	**STATISTICAL SIGNIFICANCE**	**TREND**	**STATISTICAL SIGNIFICANCE**
Winter (12, 1, 2)	**Increase**	R^2 = 0.14 p = 0.021 F(1,17) = 5.79	***NS***	R^2 = 0.13 p = 0.12
Spring (3, 4, 5)	***NS***	R^2 = 0.03 p = 0.33	**Increase**	R^2 = 0.45 p = 0.002 F(1,17) = 13.01
Summer (6, 7, 8)	***NS***	R^2 = 0.08 p = 0.089	**Increase**	R^2 = 0.60 p < 0.003 F(1,18) = 25.08
Fall (9, 10, 11)	***NS***	R^2 = 0.004 p = 0.69	**Increase**	R^2 = 0.38 p = 0.008 F(1,16) = 9.30

Table 3. Secondary winds. For Bodega Bay, east-northeast to east-southeast (67.5–112.5°) were the second most frequent wind bearings and predominated in some months. For Point Reyes G Ranch, east to south (90–180°) were the second most frequent wind bearings. “Increase” indicates a rise in the proportion of winds from a given bearing over time, “Decrease” indicates a decline, and “***NS***” indicates no statistical significance.

	BODEGA BAY ENE-ESE 67.5–112.5°		**POINT REYES G RANCH E-S 90–180°**	
SEASON (MONTHS)	**TREND**	**STATISTICAL SIGNIFICANCE**	**TREND**	**STATISTICAL SIGNIFICANCE**
Winter (12, 1, 2-)	***NS***	R^2 = 0.04 p = 0.22	***NS***	R^2 = 0 p < 0.94
Spring (3, 4, 5)	***NS***	R^2 = 0 p = 0.99	***NS***	R^2 = 0.06 p = 0.32
Summer (6, 7, 8)	***NS***	R^2 = 0 p = 0.58 F(1,15) = 19.16	**Decrease**	R^2 = 0.33 p < 0.009 F(1,18) = 8.67
Fall (9,10,11)	***NS***	R^2 = 0.01 p = 0.51	***NS***	R^2 = 0.05 p = 0.37

Table 4. Diablo winds are associated with a northeast wind direction (approximately 22.5–112.5°). "Increase" indicates a rise in the proportion of winds from a given bearing over time, "Decrease" indicates a decline, and "***NS***" indicates no statistical significance. A statistically significant change in the proportion of winds associated with Diablo wind bearings was observed in only two months.

SEASON (MONTHS)	BODEGA BAY—NNE-ESE 22.5–112.5°		POINT REYES G RANCH—NNE-ESE 22.5–112.5°	
	TREND	**STATISTICAL SIGNIFICANCE**	**TREND**	**STATISTICAL SIGNIFICANCE**
January (1)	***NS***	T = −0.14 p = 0.24	**Decrease**	T = −0.09 p = 0.0037 F(2,83) = 11.93
November (11)	***NS***	T = 0.03 p = 0.80	**Increase**	T = 0.06 p = 0.0425

Table 5. Summary of precipitation trends and extreme events at Bodega Bay and Point Reyes G Ranch. For Bodega Bay there was no evidence of a change in extreme precipitation events regarding the number of 24-hour periods where the 99th percentile was surpassed, change in the 99th percentile, or (as seen in Table 1) change in total precipitation per year. However, over the average 24-hour period during which precipitation occurred there was a significant decline in rainfall by 0.2 inches (Appendix A). "***NS***" indicates no statistical significance.

PRECIPITATION	BODEGA BAY		POINT REYES G RANCH	
	TREND	**STATISTICAL SIGNIFICANCE**	**TREND**	**STATISTICAL SIGNIFICANCE**
total days of precip.	***NS***	T = −0.08 p = 0.51	***NS***	T = 0.28 p = 0.19
99th percentile / 24 hours	***NS***	T = −0.11 p = 0.404	***NS***	T = −0.32 p = 0.06
99th percentile value	***NS***	T = −0.10 p = 0.39	***NS***	T = −0.32 p = 0.06
mean precip. / 24 hours	**Negative Correlation**	R^2 = 0.21 p = 0.004 ($F_{1,36}$ = 9.71)	**Positive Correlation**	R^2 = 0.23 p = 0.037 ($F_{1,17}$ = 5.14)
mean precip.	–	39 in	–	26.2 in
mean precip. / 24 hours	–	0.27 in	–	0.21 in
99th percentile precip.	–	1.4 in	–	1.31 in
days of precip. > 0.01 in	–	45.7 days	–	79.3 days

Atmospheric Conditions

Ambient Temperatures

Yearly mean air temperature increased at a rate of 0.16°F per year at Point Reyes G Ranch between 2006 and 2025 (F(1,15) = 14.4 p < 0.001, R^2 = 0.49). Mean maximum daily temperatures increased by 0.29°F per year (R^2 = 0.71, F(1,17) = 41.3, p < 0.00001; or 0.35°F per year based on Sen's slope estimate; Table 1, Figure 3). Mean minimum daily temperatures also exhibited a positive slope with a 0.17°F per year increase (R^2 = 0.32, F(1,17) = 8.0, p = 0.012; Figure 3). Sen's slope estimate was statistically insignificant for mean minimum daily temperature. While no significant trend was established at Bodega Bay (Figure 3), over this same period, there was a significant increase in recorded incidents in which temperatures exceeded the 99th percentile at both Bodega Bay and Point Reyes, 66°F and 82°F respectively (Figures 4 and 5; Bodega Bay, a Mann–Kendall test: tau = 0.29, p = 0.036, Point Reyes, tau = 0.48, p < 0.01).

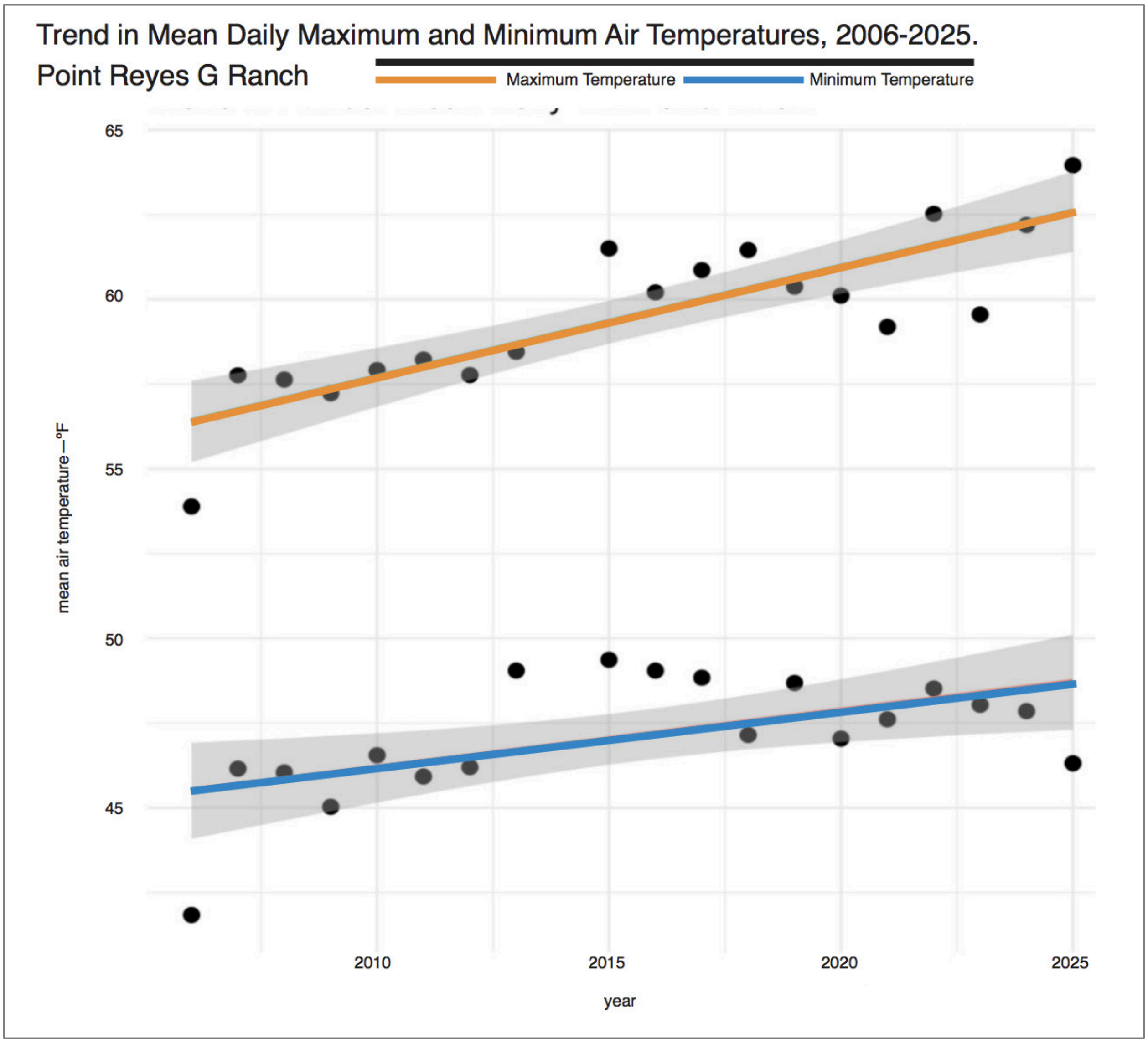

Figure 3. Trend in mean daily maximum and minimum air temperatures, 2006–2025, Point Reyes G Ranch. Maximum temperatures: $R^2 = 0.71$, $F(1,17) = 41.3$, $p < 0.00001$, Mann–Kendall test: tau = 0.65, p = 0.00012, Sen's slope estimate = 0.35°F per year, regression slope = 0.29°F per year. Minimum temperatures: $R^2 = 0.32$, $F(1,17) = 8.0$, $p = 0.012$, Mann–Kendall test: tau = 0.29, p = 0.09, Sen's slope estimate = 0.13°F per year. Regression slope = 0.16°F per year. 95% confidence intervals indicated in gray.

NPS / GREGORY ARENA

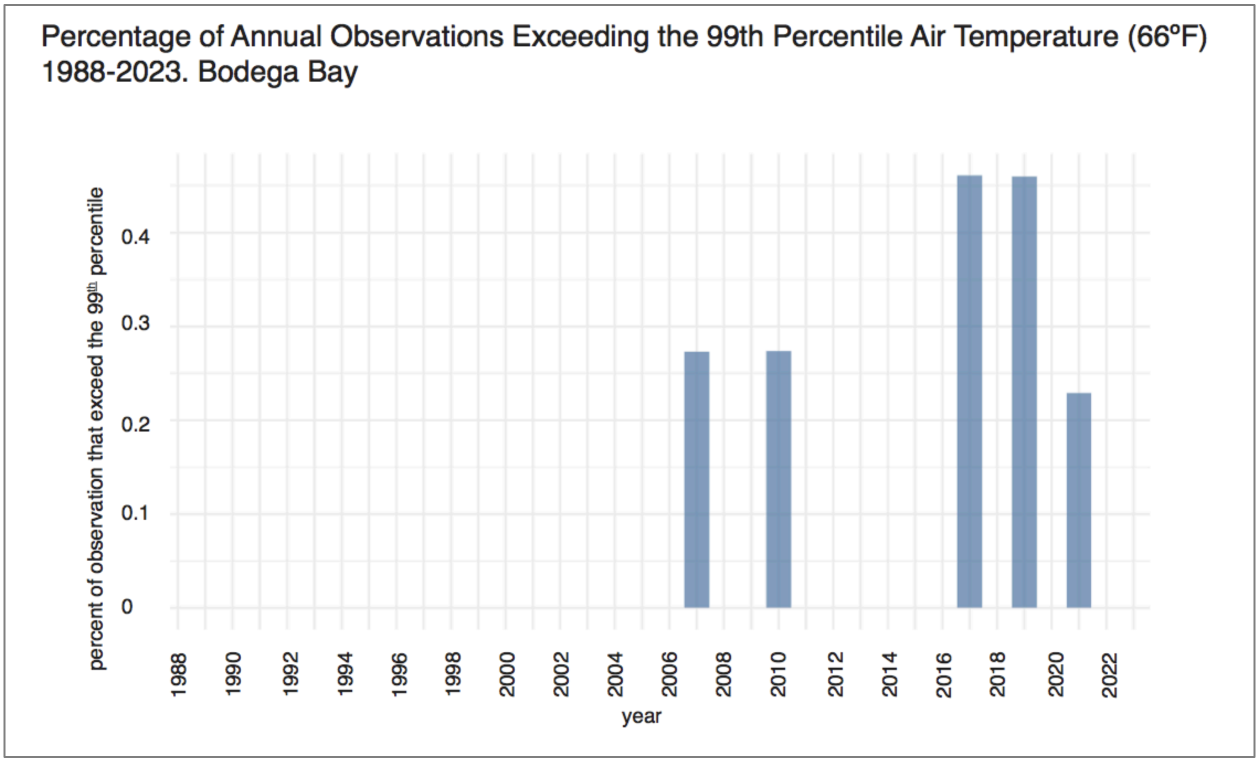

Figure 4. Percentage of annual observations exceeding the 99th percentile air temperature 1988–2023, Bodega Bay. The change in 99th percentile heat events based on present-day 99th percentile events reflected an $R^2 = 0.13$, $F(1,34) = 5.15$, $p = 0.0298$, Mann–Kendall test: tau = 0.29, $p = 0.0362$, Sen's slope estimate = 0.40% increase per year.

NPS / GREGORY ARENA

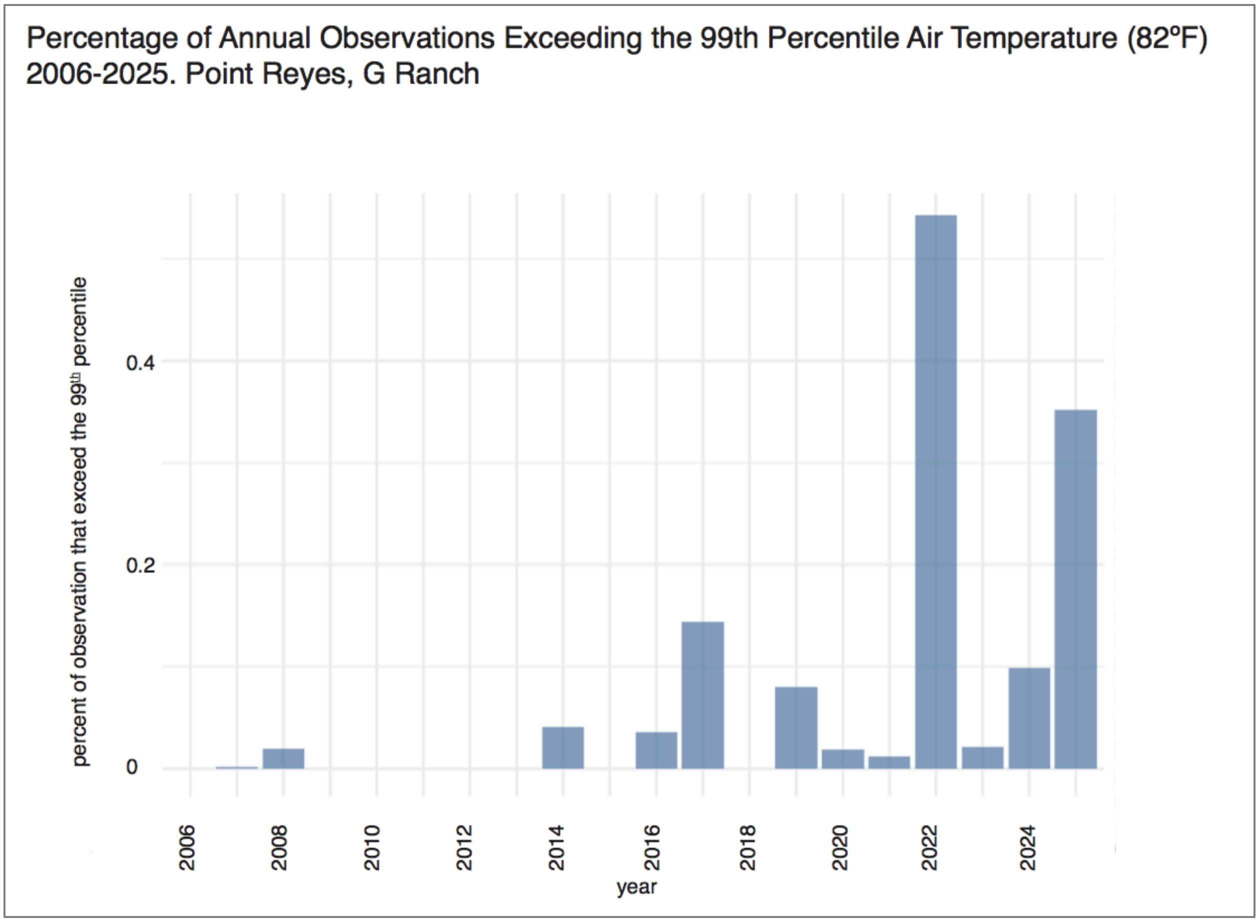

Figure 5. Percentage of annual observations exceeding the historical 99th percentile air temperature 2006–2025, Point Reyes G Ranch. A Mann–Kendall test indicated a significant, positive trend (tau = 0.48, p = 0.00526).

NPS / GREGORY ARENA

Precipitation

Average precipitation for Bodega Bay for a 24-hour period was 0.27 inches, with 1.47 inches being the average 99th percentile for precipitation within a 24-hour period with a mean annual precipitation of 39 inches (Table 5). Average precipitation for Point Reyes G Ranch for a 24-hour period was 0.21 inches, with 1.31 inches being the average 99th percentile for precipitation within a 24-hour period with a mean of 26.2 inches of rain annually. For Bodega Bay, there was a significant decline in the amount of precipitation within a 24-hour period between 1988 and 2025 (Regression $R^2 = 0.21$, $F(1,36) = 9.71$, $p = 0.003$, Mann–Kendall test: tau = −0.31, $p = 0.007$). For Point Reyes G Ranch, there was a significant increase in the amount of precipitation within a 24-hour period between 2006 and 2025 (Regression $R^2 = 0.23$, $F(1,17) = 5.14$, $p = 0.04$, Mann–Kendall test: tau = 0.47, $p = 0.005$; Appendix A). For both sites, there was no significant change in the number of precipitation events that exceeded the 99th percentile. There was also no significant change in the 99th percentile per year (Table 5). Furthermore, there was no statistically significant trend in precipitation over time, by season, month, or year.

VPD and Relative Humidity

Between 1988 and 2025, there was a statistically significant decline in VPD at Bodega Bay during June through August (Figure 6). A linear regression plotted a decline of 0.002 kPa per year (R^2 = 0.21, F(1,32) = 8.74, p = 0.0058), while a Mann–Kendall test (tau = −0.2676, p = 0.027) provided a Sen's slope estimate of a 0.0037 kPa yearly decline in VPD. There was a statistically significant positive relationship between RH and time (Figure 7). A linear regression (R^2 = 0.19, F(1,31) = 7.3, p = 0.011) indicated an increase by 0.13% per year, while a Mann–Kendall test (tau = 0.2332, p = 0.05869) proposed a 0.365% increase in RH per year since 1988. There was insufficient data to establish a significant trend for either VPD or RH at Point Reyes G Ranch (Table 1). Mean VPD for June through August was 0.16 kPa at Point Reyes G Ranch, and 0.07 kPa at Bodega Bay.

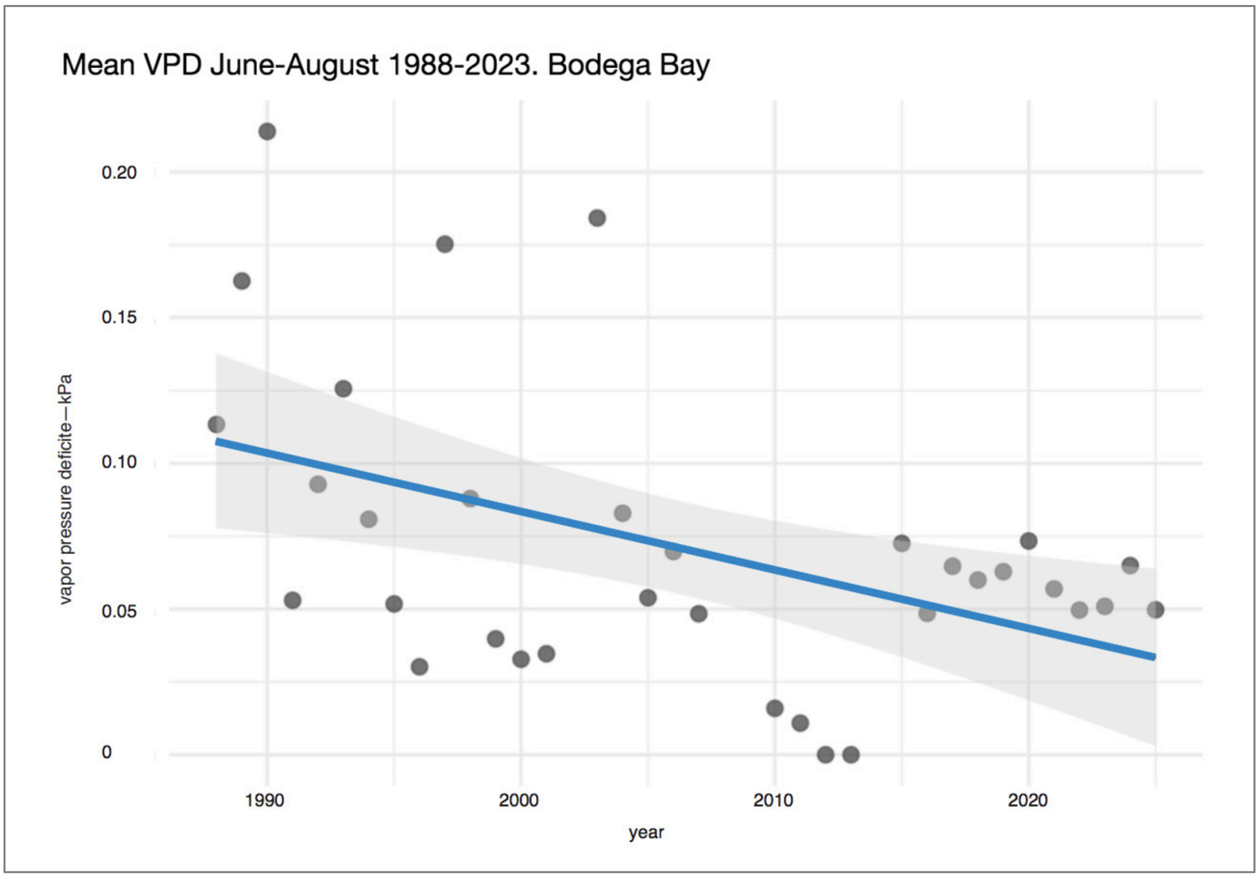

Figure 6. Mean June–August VPD at Bodega Bay, 1988–2023. VPD = 4.0983 − 0.002 × year, R^2 = 0.25, F(1,32) = 8.7393, p = 0.00581. Mann–Kendall test: tau = −0.27, p = 0.0272, Sen's slope estimate = −0.0037 kPa per year. The mean June–August VPD at Bodega Bay during 1988–2023 was 0.07 kPa. While no trend could be established for Point Reyes G Ranch, the mean VPD was 0.16 kPa. The gray shaded area represents the 95% confidence interval around the fitted regression line.

NPS / GREGORY ARENA

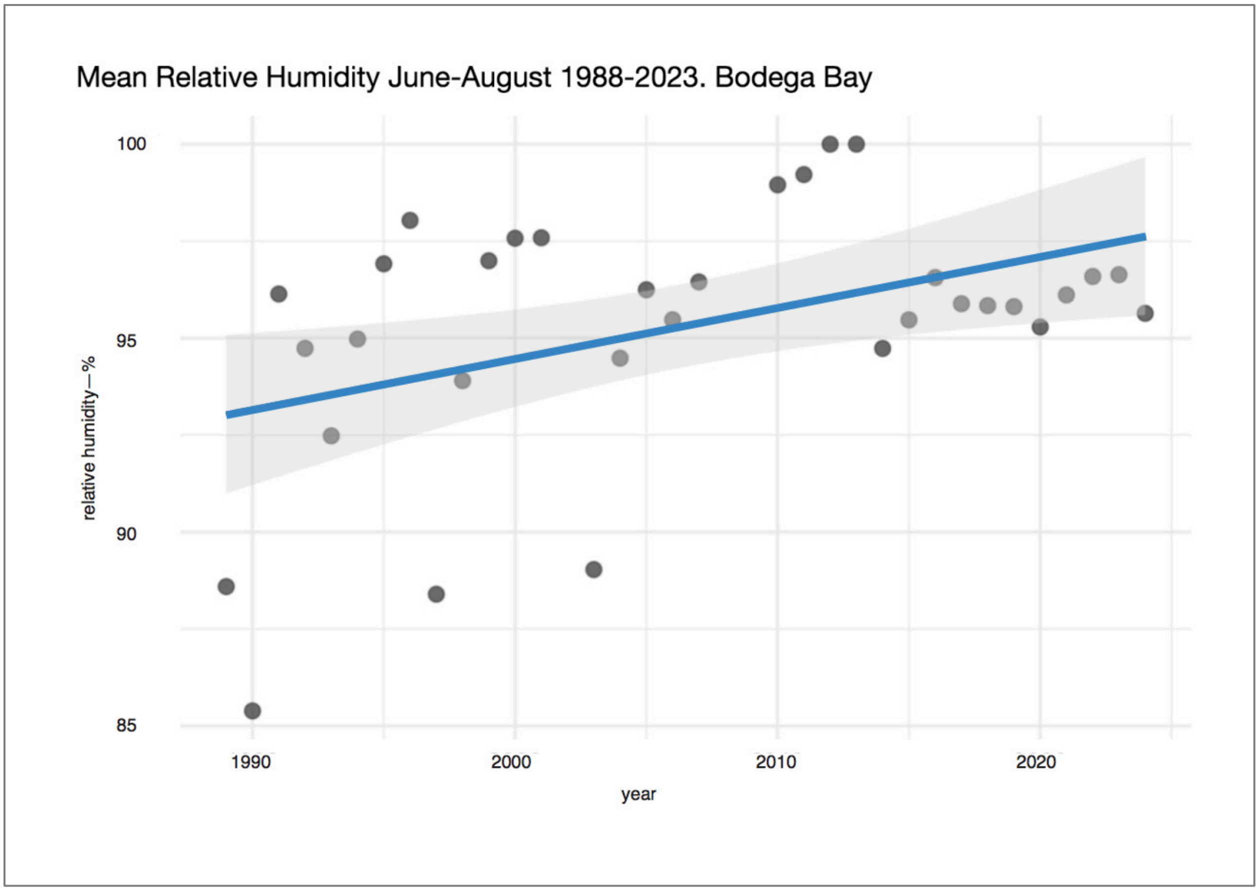

Figure 7. Mean relative humidity June–August, 1988–2023, Bodega Bay. RH = −167.7805 + 0.1311 × year, $R^2 = 0.19$, $F(1,31) = 7.31$, $p = 0.0110$, Mann–Kendall test: tau = 0.23, $p = 0.0587$, Sen's slope estimate = 0.3592% in RH per year. 95% confidence intervals indicated in gray.

NPS / GREGORY ARENA

Wind Speed

There was no statistically significant change in wind speed over time at either Bodega Bay or Point Reyes G Ranch (Table 1). At Point Reyes G Ranch, there was no relationship most of the year between wind speed and RH. During winter and spring, within months and specific times of day there were instances where either positive or negative relationship could be identified, but none of these trends appeared consistent. June through August represented the only period during which there was a consistent negative relationship between wind speed and RH ($F(1,17896) = 99.51$ $p < 0.007$) between all RH bins, excluding 80–90% and 90–100% ($p > 0.1$; Figure 8).

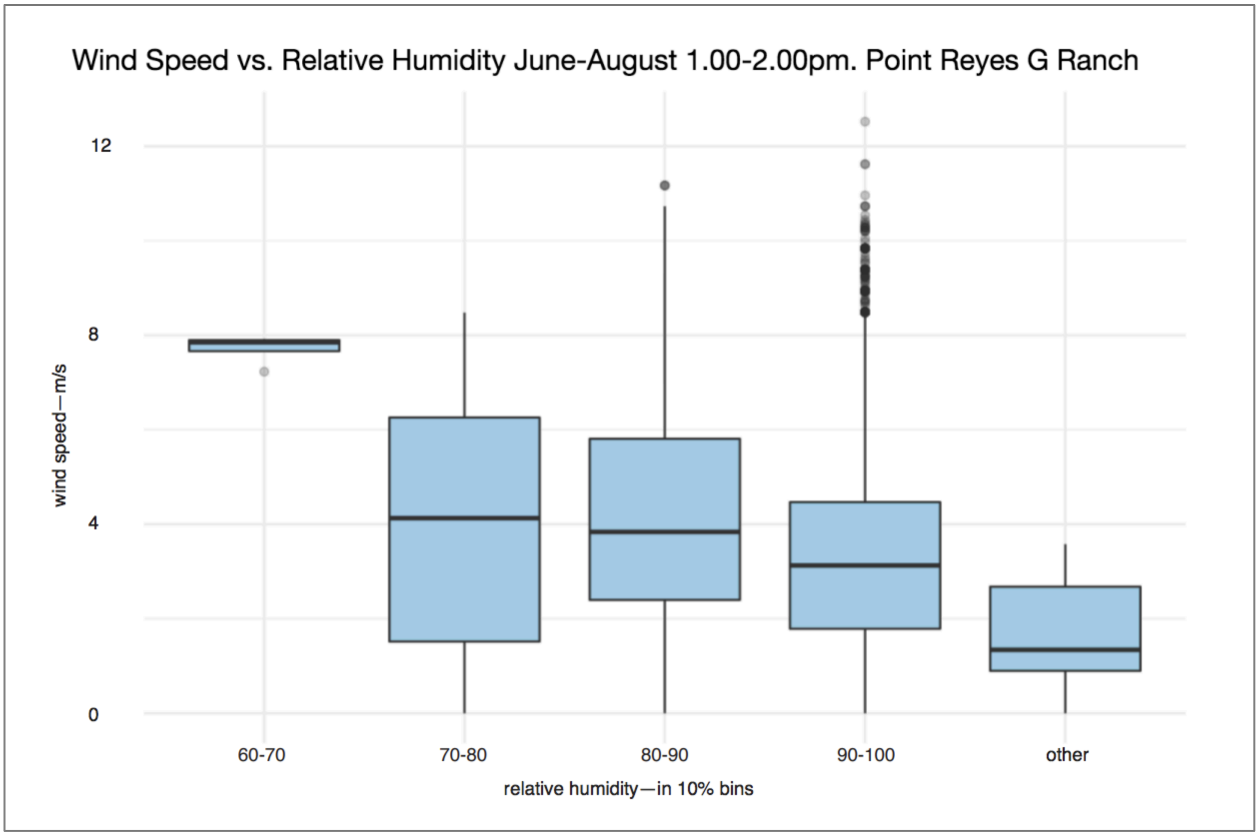

Figure 8. Wind speed vs. relative humidity June–August at Point Reyes G Ranch. $F(1,17896) = 99.51$, $p < 0.007$ between all RH bins except between bin 80–90% and 90–100% ($p = 0.999$). The category designated "other" accounts for RH observations between 0 and 59%. These observations account for only 3.88% of all observations considered in this analysis and were not statistically significant when compared with other bins. Values below 59% may reflect sensor errors, or anomalous weather patterns. *NPS / GREGORY ARENA*

Wind Direction

For Point Reyes G Ranch, wind with a West Northwest (292.5°) to North (360°) bearing predominated in all months and accounted for greater than 30% of all observations combined (Appendix A). This overall trend was mirrored at Bodega Bay with the exceptions of January and December where East (90°) and East Southeast (112.5°) bearings were most observed (Appendix A). There was no statistically significant variation in wind direction between 1988 and 2025 for Bodega Bay with the exception of an increase in wind with a bearing NW to N (315–360°) between the months of December and February ($R^2 = 0.14$, $F(1,36) = 5.61$, $p = 0.0214$). For Point Reyes G Ranch, there was a significant increase in wind with a NWN to N bearing between the months of March and November. This trend was greatest in June through August ($R^2 = 0.59$, $F(1,18) = 25.0$, $p = 0.000107$; Figure 9). During June through August, there was also a decline in wind with an E to SE bearing (90–180°; $R^2 = 0.59$, $F(1,18) = 25.0$, $p = 0.0001$). There was a statistically significant change in the proportion of wind with an E or NE bearing in January (tau = −0.089, $p = 0.004$) and November (tau = 0.064, $p = 0.042$; Table 2). For Point Reyes G Ranch, from March through May there was a correlation between wind direction and precipitation, with more precipitation coming from 240° relative to 280° (Figure 10).

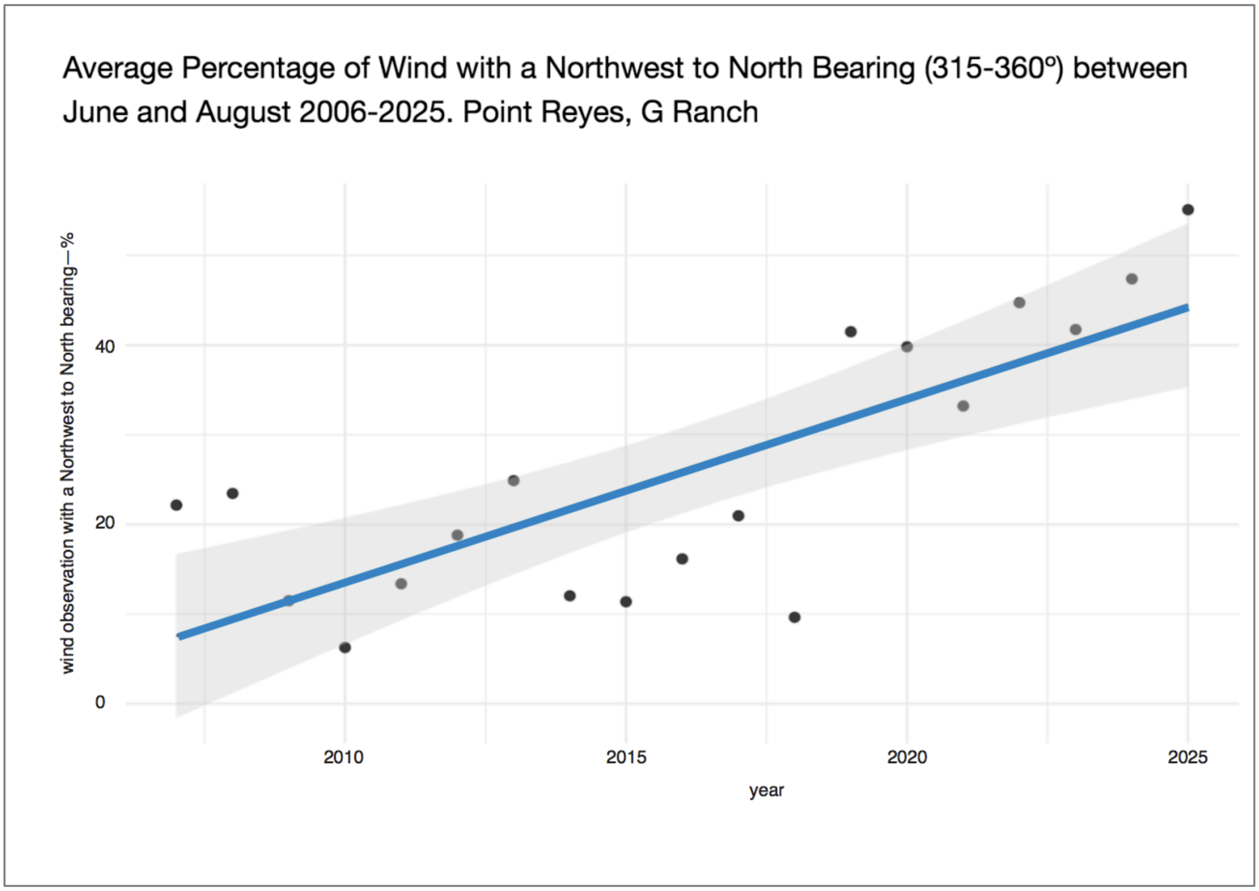

Figure 9. Average percentage of wind with a northwest to north bearing June–August, 2006–2025, Point Reyes G Ranch. $R^2 = 0.596$, $F(1,18) = 25.08024$, $p = 0.000107$, Mann–Kendall test: tau = 0.509, $p = 0.0026232$, Sen's slope estimate = 2.132231% increase in observations per year. 95% confidence intervals indicated in gray.
NPS / GREGORY ARENA

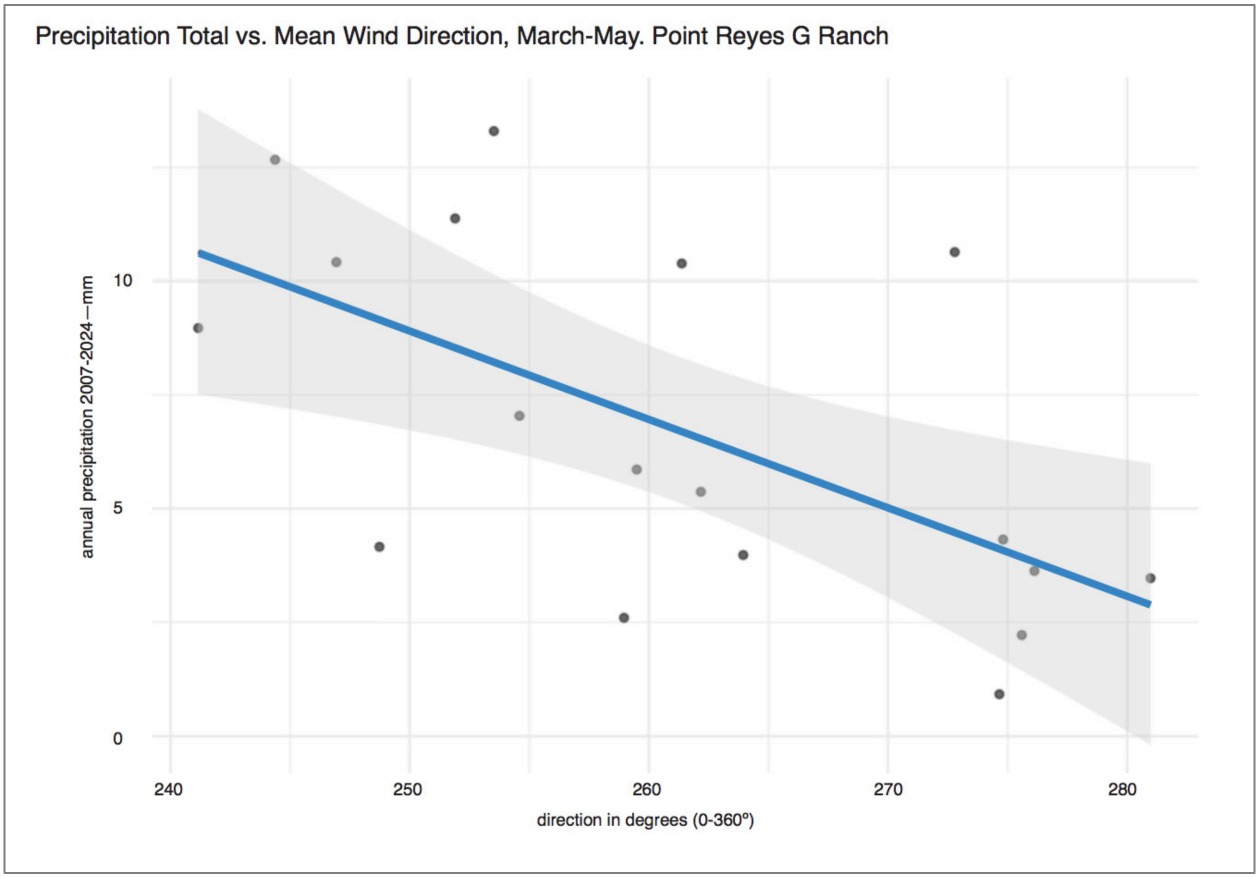

Figure 10. Precipitation total vs. mean wind direction March–May at Point Reyes G Ranch. R^2 = 0.37, F(1,16) = 9.476, p = 0.0072. 95% confidence intervals indicated in gray.
NPS / GREGORY ARENA

Solar Radiation and Cloud Coverage

At both Bodega Bay and Point Reyes G Ranch, there was a negative relationship between solar radiation and time (Figures 11 and 12). At Bodega Bay between 1988 and 2025 the relationship was characterized by an $R^2 = 0.56$, $F(1,15) = 90.4$, $p < 0.001$ and a Sen's slope estimate = −0.12. At Point Reyes G Ranch there is a slight downward trend in solar radiation (tau = −0.093, p < 2.22e-16) between 2019 and 2025 when DRI collected solar radiation data. For both Bodega Bay and Point Reyes G Ranch, there was a positive relationship between wind speed and solar radiation during the summer months (Bodega Bay, 2.00 pm, July $R^2 = 0.56$, F(1 ,1109) = 134, p < 1.4e-27; Point Reyes G Ranch, 12.00 pm, July $R^2 = 0.1401$, F(1,2890) = 471, p < 2.2e-16; Figures 13 and 14).

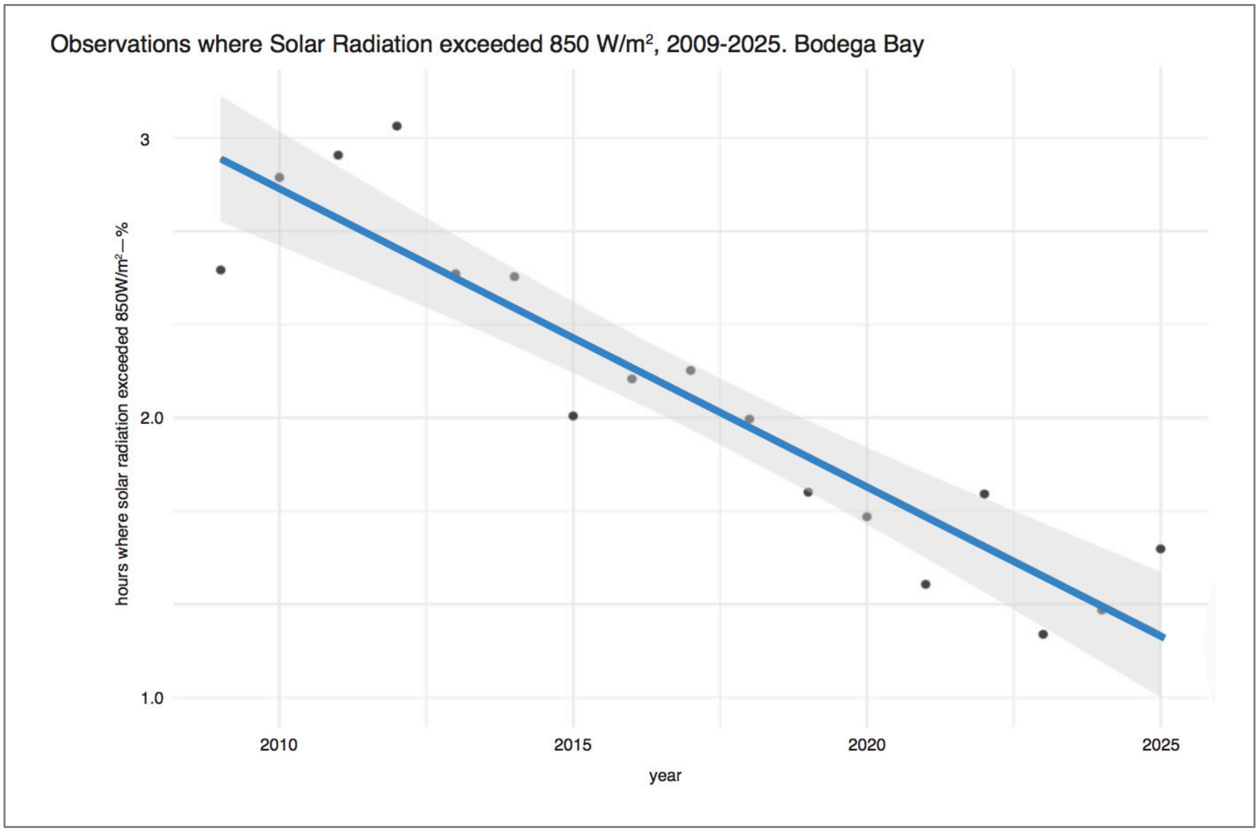

Figure 11. Observations where solar radiation exceeded 850 W/m^2, 2009–2025, Bodega Bay. $R^2 = 0.86$, $F(1,15) = 90.4$, $p < 0.00001$, Mann–Kendall test: tau = −0.78, $p < 0.00001$, Sen's slope estimate = −0.16. 95% confidence intervals indicated in gray.

NPS / GREGORY ARENA

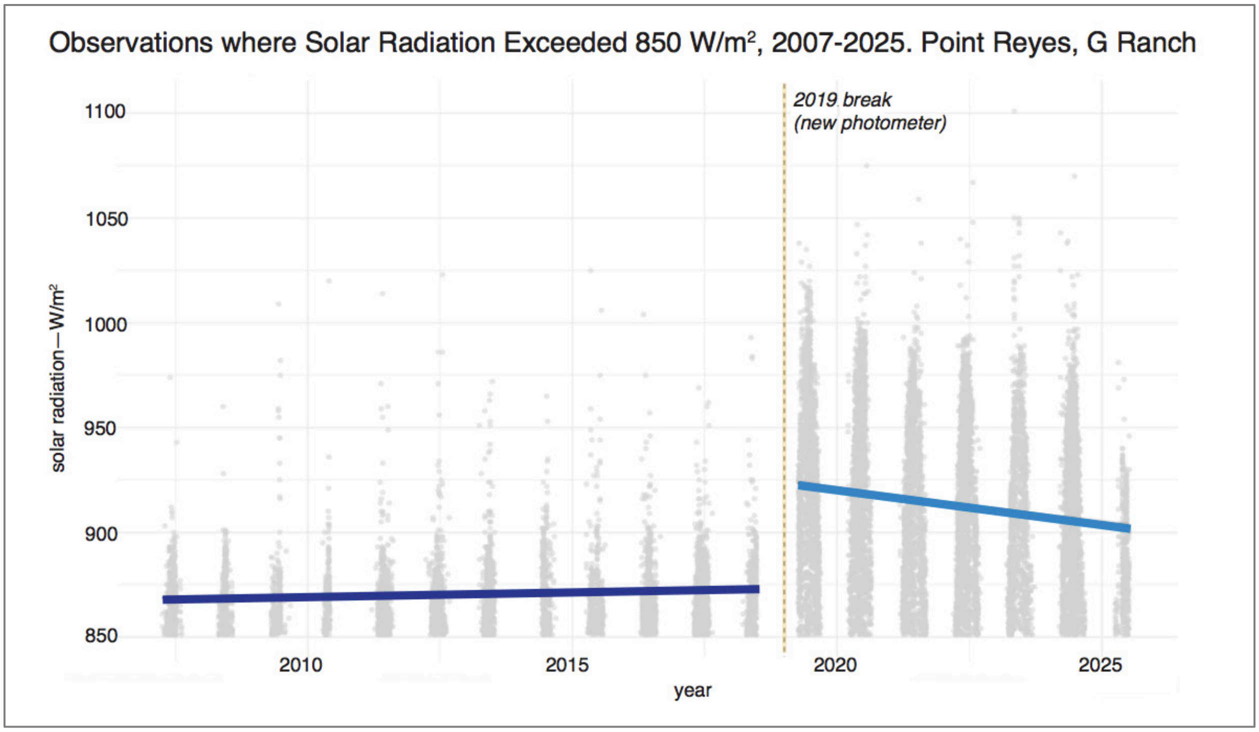

Figure 12. Observations where solar radiation exceeded 850 W/m^2, 2007–2025, Point Reyes G Ranch. For both regressions, the $R^2 < 0.01$, though significant ($p < 0.0001$). $F(3,25291) = 1953$, Mann–Kendall test: tau = 0.060, $p < 2.22e-16$ for 2007–2019, and tau = −0.0928, $p < 2.22e-16$ for 2019–2025. 2019 marks the date when the sensor was replaced. 95% confidence intervals for regression lines are shown in gray.

NPS / GREGORY ARENA

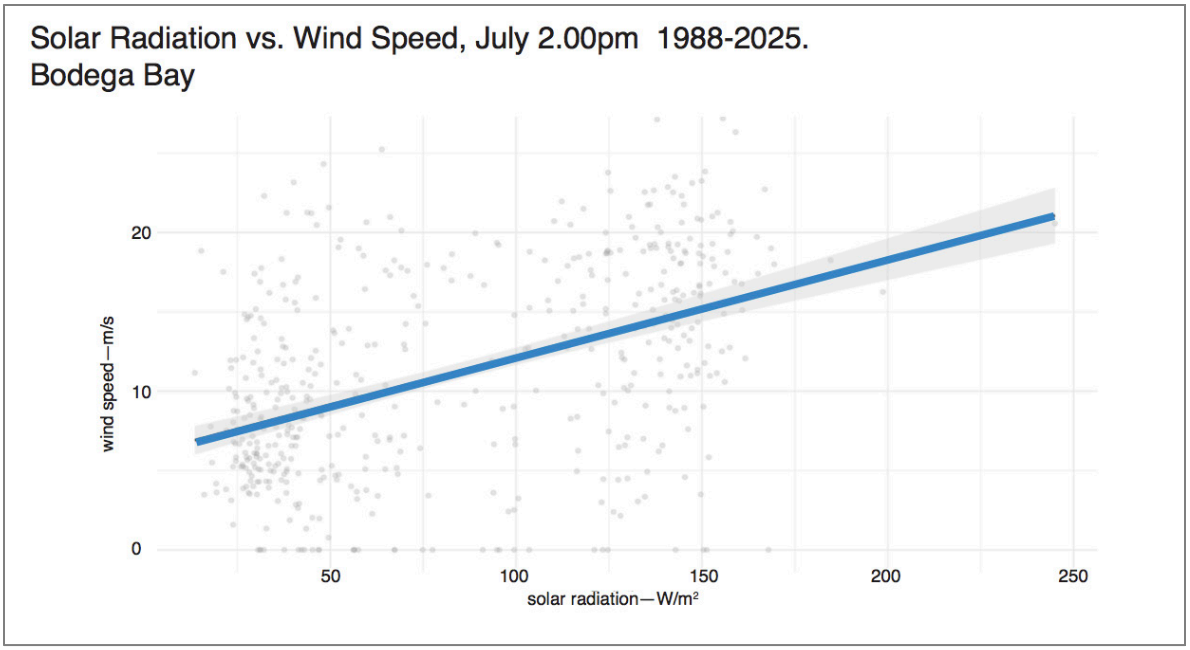

Figure 13. Solar radiation vs. wind speed, July 1988–2025, Bodega Bay. $R^2 = 0.56$, $F(1,1109) = 134$, $p < 0.000001$, Mann–Kendall test: tau = 0.072, $p = 0.017$, Sen's slope estimate = 0.005. 95% confidence intervals indicated in gray.

NPS / GREGORY ARENA

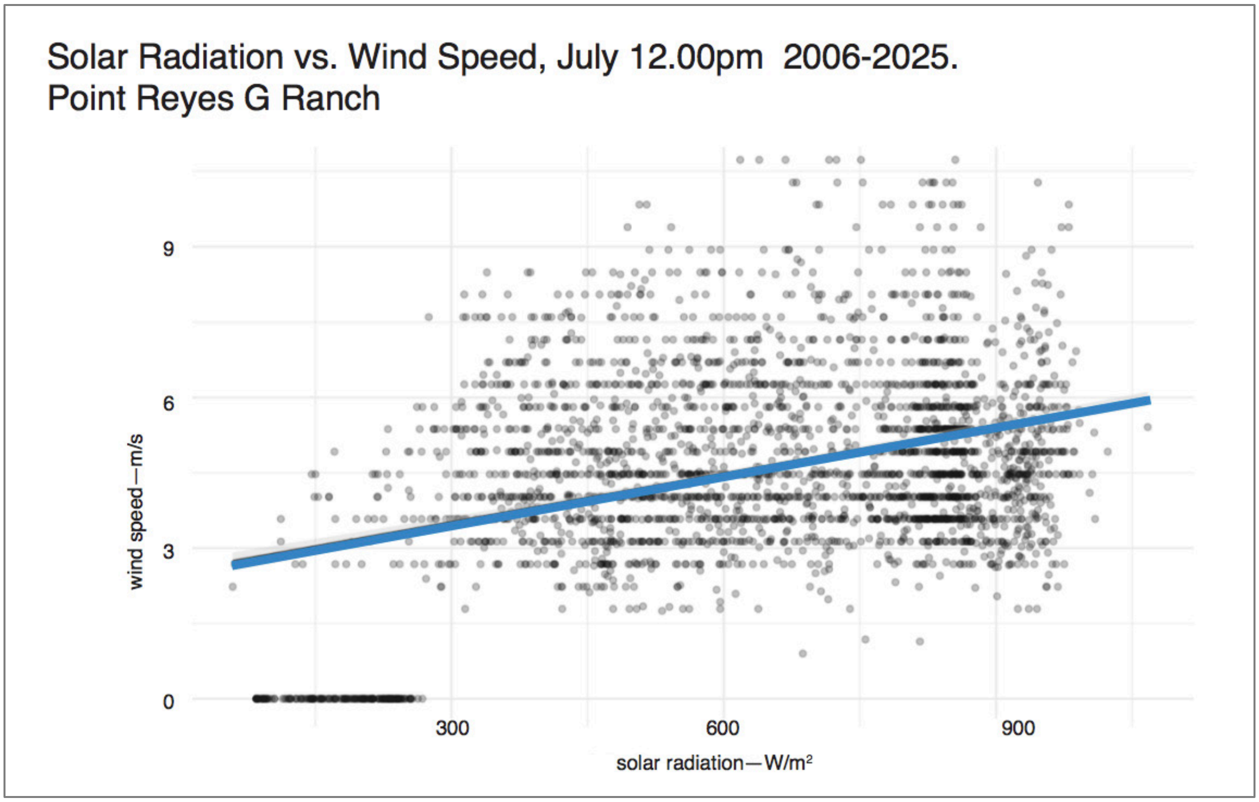

Figure 14. Solar radiation vs. wind speed, July 2006–2025, Point Reyes G Ranch. $R^2 = 0.14$, $F(1,2890) = 470$, $p < 0.0001$, Mann–Kendall test and Sen's slope estimate $p > 0.05$. 95% confidence intervals indicated in gray.

NPS / GREGORY ARENA

Soil Conditions

Average soil maximum and minimum temperatures at Point Reyes G Ranch decreased slightly between 2021 and 2025, June through August (Regression $R^2 = 0.51$, $F(1,405)$: 416.2, $p < 0.00001$, Mann–Kendall test: tau = −0.38, $p < 0.00001$, Sen's slope estimate = −0.018°F per year. Minimum temperatures: Regression $R^2 = 0.40$, $F(1,405) = 275.1$, $p < 0.00001$, Mann–Kendall test: tau = −0.33 $p < 0.00001$, Sen's slope estimate = −0.012°F per year; Figure 15). Over this same time period, there was a declining amplitude between summer highs and winter lows ($R^2 = 1$, $F(1,51) = 17{,}840$, $p <$ 2.2e-16; Figure 16). At Point Reyes G Ranch, there was also a negative correlation between soil temperature and soil moisture ($R^2 = 0.55$, $F(1,3682)$ = 4.509e+04, $p <$ 2.2e-16; Figure 17). At Point Reyes G Ranch between 2021 and 2025 (when these data were recorded), there was a significant increase in soil moisture ($R^2 = 0.11$, $F(1,225052)$ = 2.794e+04, $p <$ 2.2e-16 (Table 1).

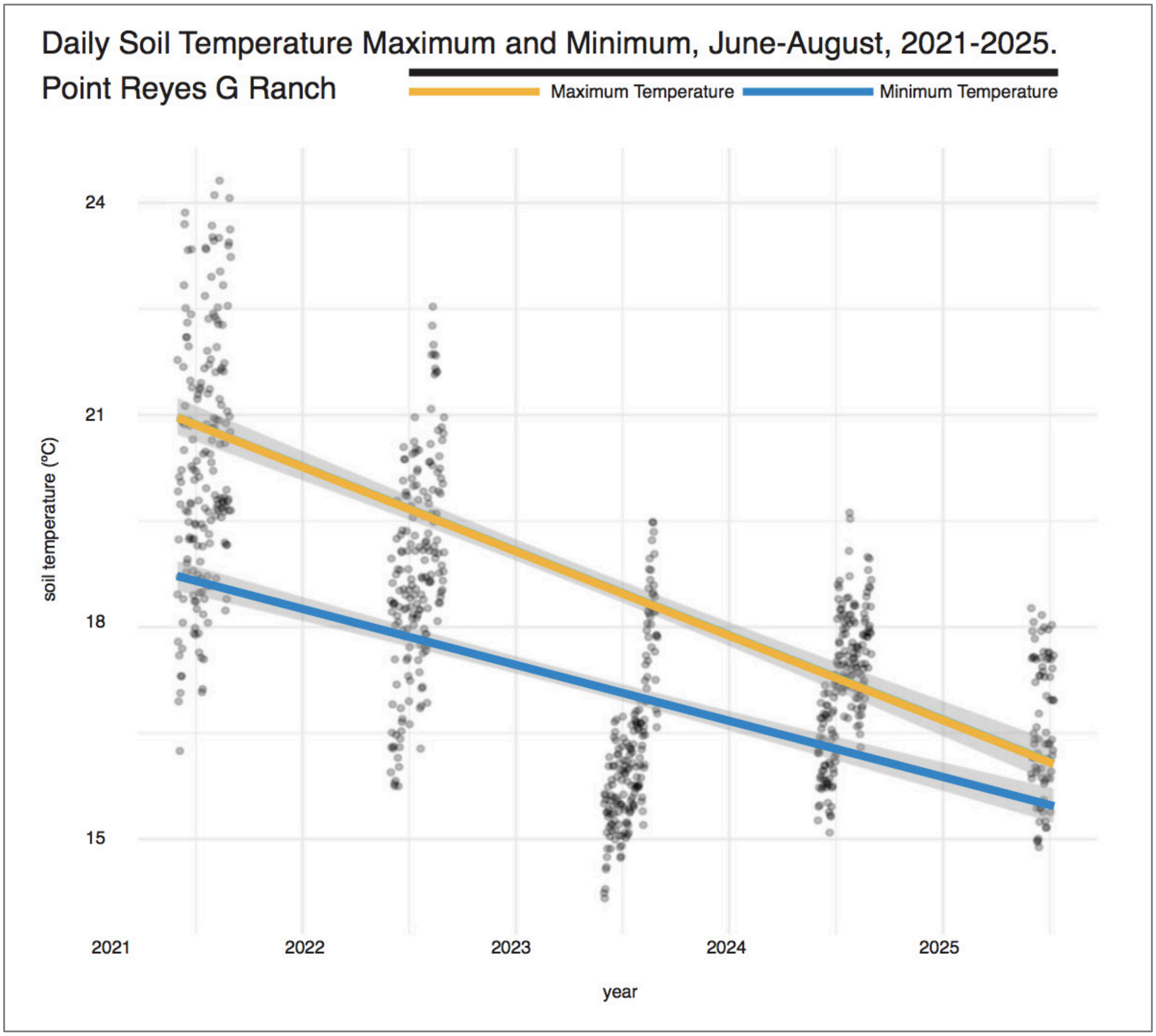

Figure 15. Daily soil temperature maximum and minimum, June–August, 2021–2025, Point Reyes G Ranch. Maximum temperatures: $R^2 = 0.51$, $F(1,405) = 416.2$, $p < 0.00001$. Mann–Kendall test: tau = −0.38, $p < 0.00001$, Sen's slope estimate = −0.018°F per year. Minimum temperatures: $R^2 = 0.40$, $F(1,405) = 275.1$, $p < 0.00001$. Mann–Kendall test: tau = −0.33, $p < 0.00001$, Sen's slope estimate = −0.012°F per year. 95% confidence intervals indicated in gray.

NPS / GREGORY ARENA

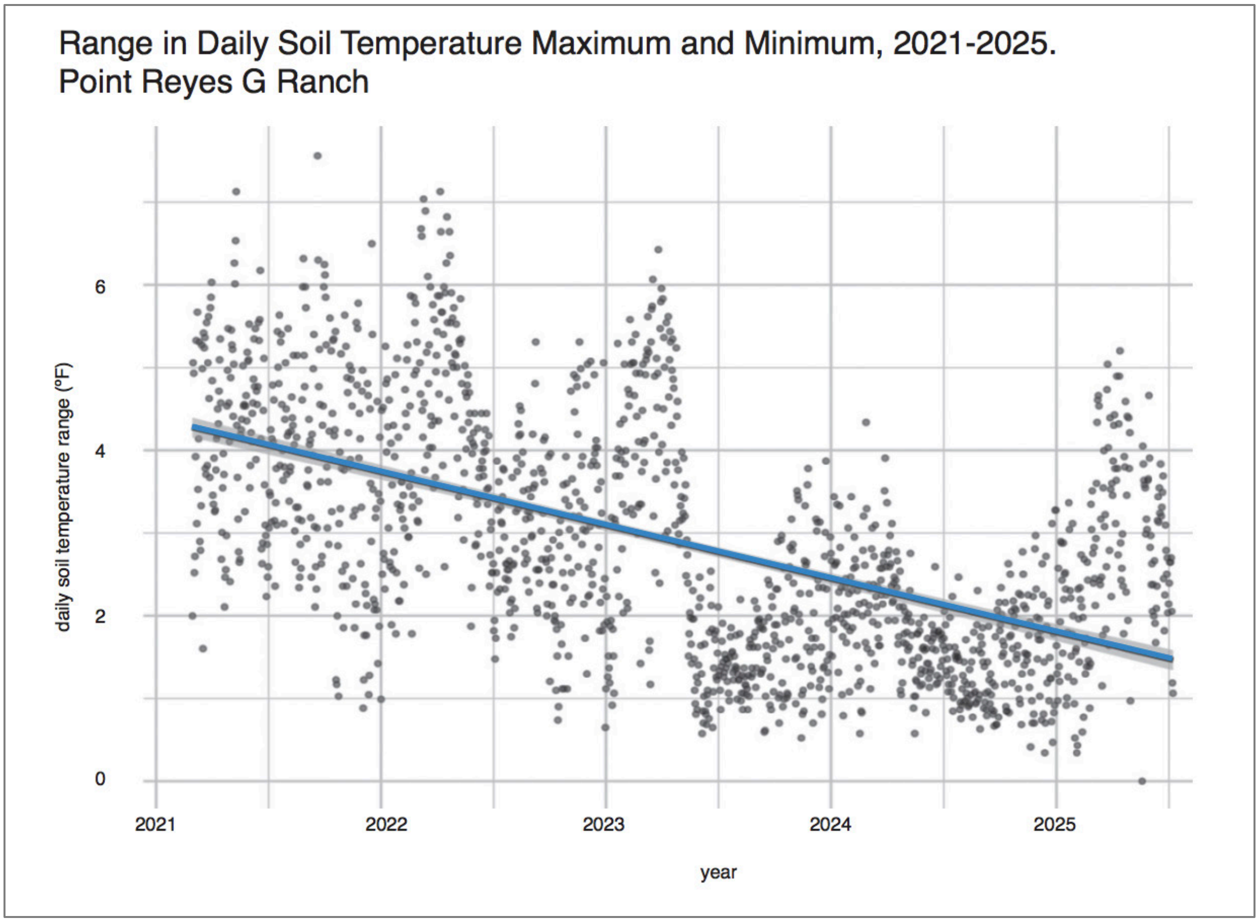

Figure 16. Range in daily soil temperature maximum and minimum, 2021–2025, Point Reyes G Ranch. $R^2 = 0.31$, $F(1,1571) = 701.5$, $p < 0.00001$. Mann–Kendall test: tau = −0.37, $p < 0.00001$, Sen's slope estimate = −0.015°F per year. 95% confidence intervals indicated in gray.

NPS / GREGORY ARENA

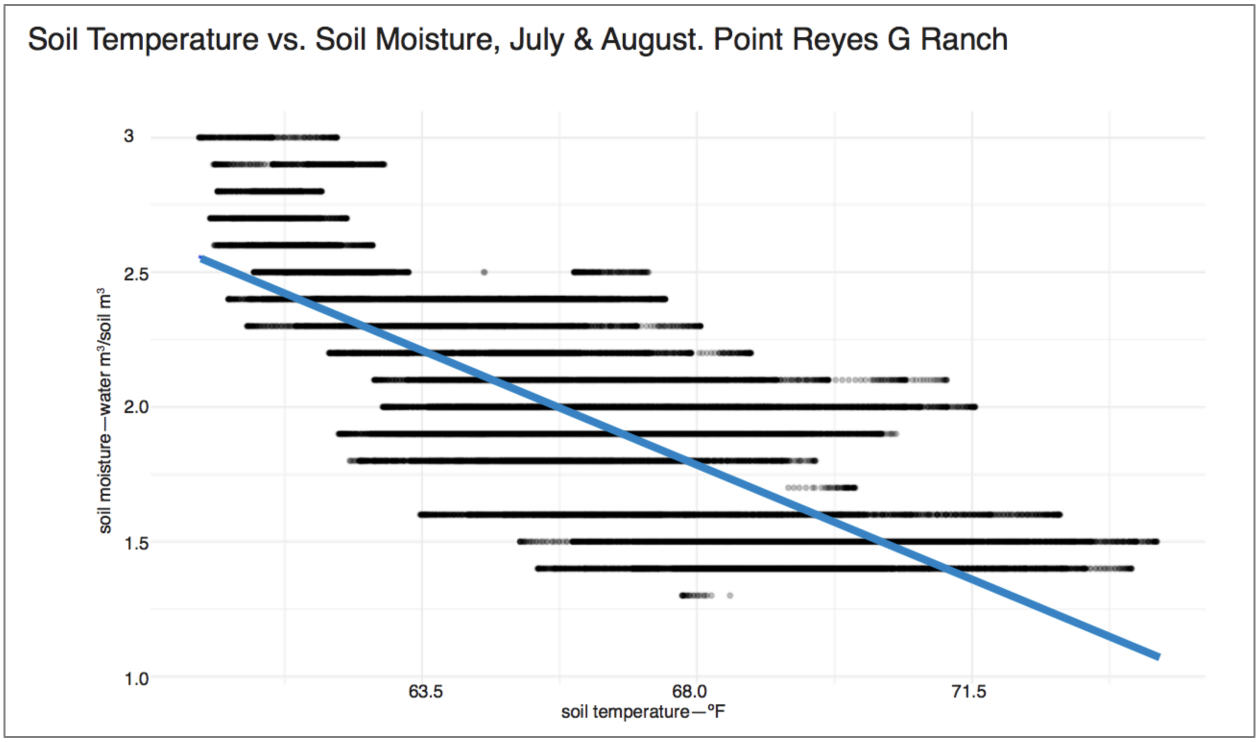

Figure 17. Soil temperature vs. soil moisture, July and August, Point Reyes G Ranch. $R^2 = 0.55$, $F(1,3682) = 4.50e+04$, $p < 2.2e-16$. 95% confidence intervals indicated in gray.
NPS / GREGORY ARENA

Discussion

Based on data collected between 1988 and 2025 at Bodega Marine Laboratory and Point Reyes National Seashore, there was evidence of significant increases in ambient temperature and/or heat events above the 99th percentile. While there was no significant change in annual precipitation, there was a slight long-term decrease in average precipitation received within a 24-hour period at BML, and a slight increase at Point Reyes G Ranch. These findings corroborate the historical climate data and trends in the Point Reyes Climate Futures Summary (CCRP 2024). A significant decline in incoming solar radiation and increase in RH suggests that maritime influences may help offset moisture loss from this system (Table 1). The data provide compelling information about the seasonal relationships between abiotic factors as they relate to water and energy balance at these coastal sites.

Atmosphere

Ambient Temperatures

Coastal areas at Point Reyes G Ranch and, to some extent, Bodega Bay have experienced warming over the last 37 years. Based on gridded historical data for the park centroid, located 2.5 miles from the Pacific Ocean and 2.25 miles from the site of the DRI met station, CCRP found a warming rate of 4.1°F per century since 1970 (CCRP 2024; Figure 2). G Ranch data aligned with these grid-based warming trends. Between 2007 and 2025, there was a statistically significant increase in annual temperatures equivalent to 0.16°F per year at G Ranch (Table 1; Figure 3). Assuming a consistent rate of warming, there will be a median +3.95°F increase by 2050 at G Ranch. Point Reyes climate futures estimate an increase in average temperatures between 1.5 and 5.1°F by 2050 (CCRP 2024; Figure 18). There was no significant trend at the Bodega Bay weather station over this same period. However, a significant increase in the number of incidents where temperatures exceeded the 99th percentile for both Bodega Bay and Point Reyes further suggest long-term warming at each site (Figures 3–5). PORE climate futures project that by 2050, the Seashore will experience between 5.6 and 15.8 days exceeding the 99th percentile for heat vs. 3.5 days per year historically. Taken together, the historical temperature data and climate futures indicate the Seashore has already experienced significant warming. That trend is likely to continue through 2050, including increases in average annual temperature and the number of extremely warm days. A warmer future may increase moisture deficit at the Seashore due to increasing evaporative demand. During water-limited periods, plants with limited water access at the Seashore may not be able to rely on sensible heat loss to offset heat. Warmer conditions and 99th percentile heat events may create acute metabolic stress for plants (Grossiord et al. 2020).

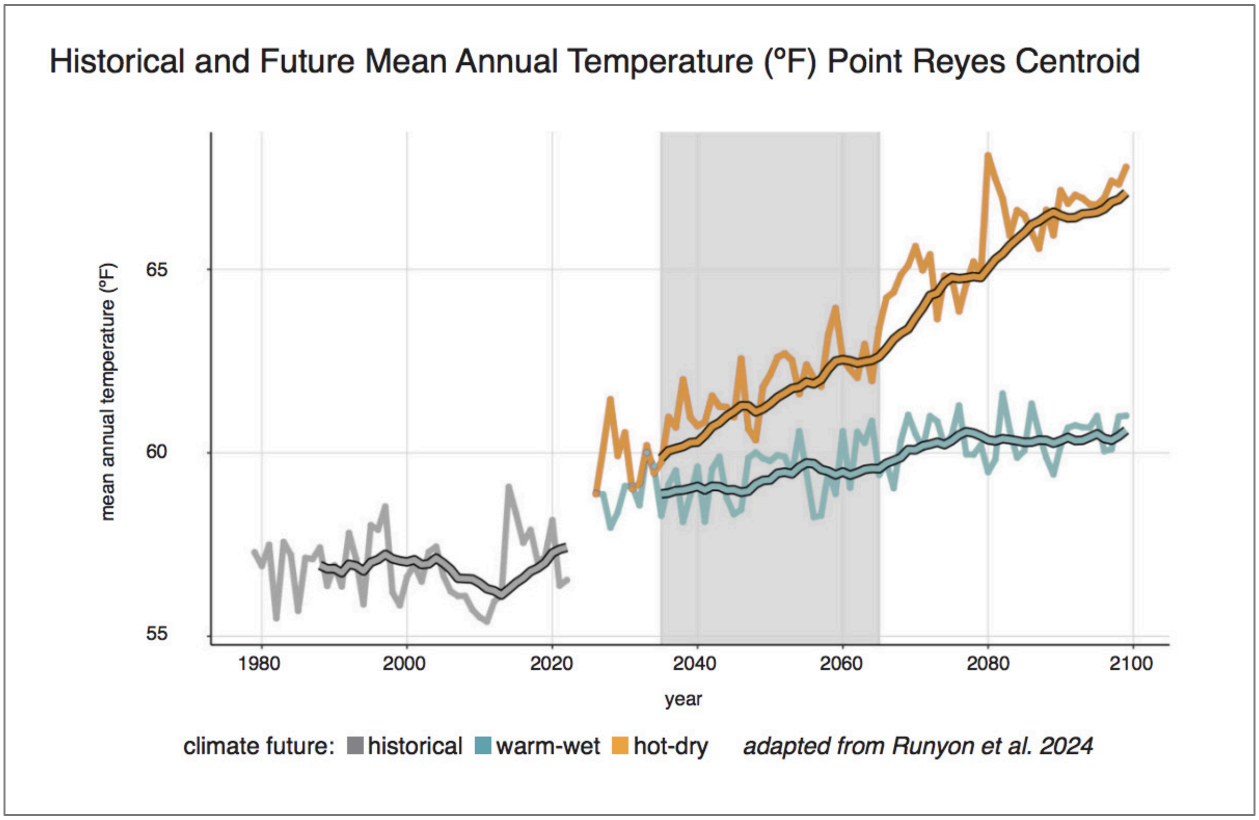

Figure 18. Comparison of observed average annual temperatures at Point Reyes against park climate futures. In grey, historical trends, 1979–2022 for climate data sourced from Bear Valley (toward the interior of the park). The orange trend line highlights a hot-dry future, while the blue line highlights a warm-wet future. Smoothed lines represent 10-year running averages.

NPS / CCRP

Precipitation

Analysis of 37 years of precipitation data from BML and 19 years of Point Reyes G Ranch data suggested no statistically significant trend in annual or monthly precipitation totals (Tables 1 and 5). Similarly, no statistically significant trend was observed using the gridded climate data for Point Reyes. However, CCRP climate change projections indicate that by 2050 the largest rainfall events may exceed 9 inches within a 24-hour period in a warm-wet future or 4.4 inches in a hot-dry future. These projections far exceed the historical 99th percentile of 2.6 inches for the park centroid (CCRP 2024; Figure 2). Coastal meteorological station data, however, do not currently align with these projections. While there was no significant change in total annual precipitation between 1989 and 2025, there was a significant decline in the average precipitation received within a 24-hour period observed for both sites. While these trends are significant, both trends are slight, with a change of no greater than 0.2 inches of precipitation per 30 years (Appendix A). Precipitation is highly variable across the Seashore, with precipitation along the immediate coast such as at G Ranch and Bodega Bay sparser than in the higher elevation sites and the coast range interior. Precipitation at the Seashore ranges from 11.5 inches/year at the coastline to 36 inches/year at Bear Valley (NPS 2024). The 99th percentile of precipitation was 1.47 inches, and 1.31 inches for Bodega Bay and Point Reyes

G Ranch, respectively. These values are far less than the 99th percentile for the park centroid (2.6 inches; Table 5, Figure 19; CCRP 2024). Given this historical data, there is little evidence that extreme precipitation along the immediate coastline will increase or produce flash flooding, or heightened erosion risk. Extreme precipitation events are characterized by a higher volume of run-off, rather than infiltration. Therefore, the decline in average precipitation within a 24-hour period in combination with no historical change in either 99th percentile events or annual precipitation totals suggests continued opportunity for precipitation to infiltrate the soil, and consistent soil moisture content and water availability for plants along the coast (Albano et al. 2020). Modeled extreme precipitation events at the park centroid may reflect more variable precipitation experienced at inland sites such as the watersheds of Olema and Lagunitas Creeks. Already, high precipitation events due to atmospheric rivers have presented risk of flooding and erosion within these basins and where there is run-off from higher elevation sites (Cordeira et al. 2019; NPS 2024).

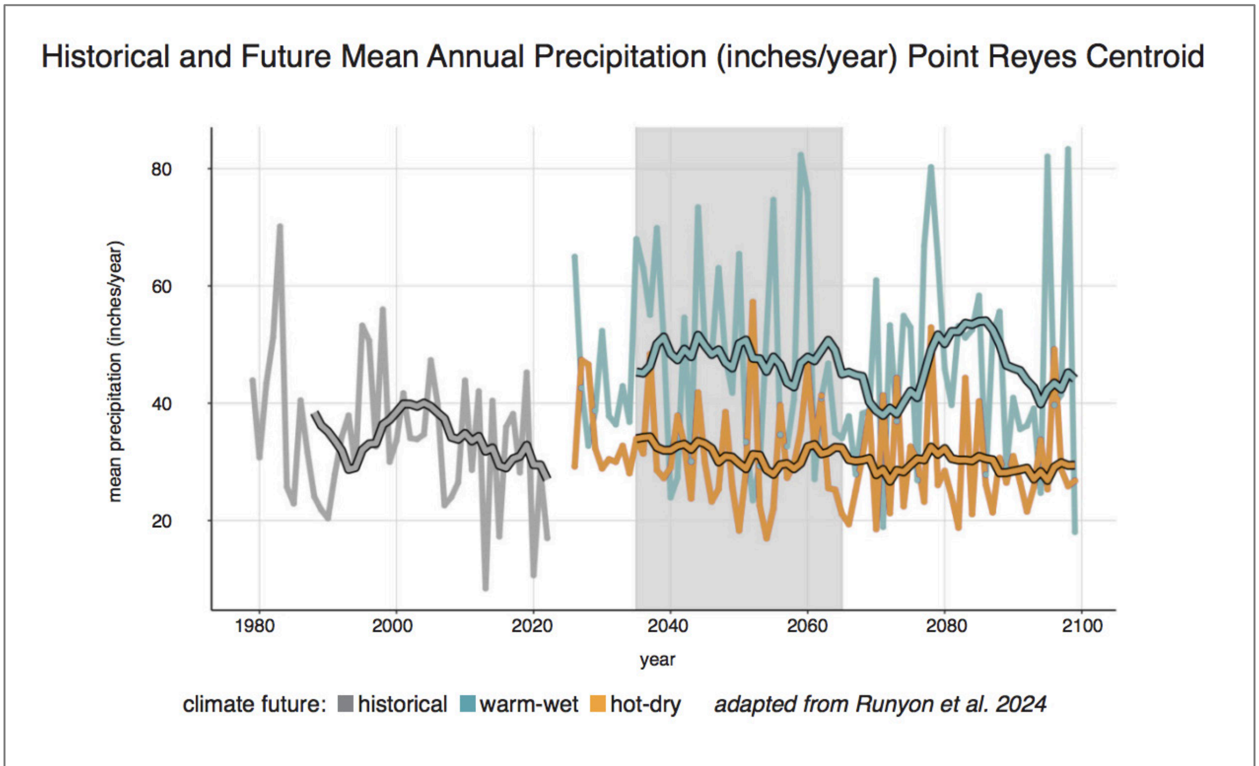

Figure 19. Comparison of observed average annual precipitation at Point Reyes with potential future precipitation. In grey, historical trends, 1979–2022 for climate data sourced from Bear Valley (toward the interior of the park). The orange trend line highlights a hot-dry future, while the blue line highlights a warm-wet future. Smoothed lines represent 10-year running averages.
NPS / CCRP

Divergent climate futures estimate a decline in precipitation at Point Reyes by as much as 5 inches (warm-wet) or an increase in annual precipitation by as much as 12 inches (hot-dry) by 2100 (CCRP 2024). This range of estimates emphasizes uncertainty in future annual precipitation. Regardless of future increase or decrease in precipitation, current models anticipate a warming climate will increase

VPD, a measure of the proportion of moisture the air can hold relative to how much moisture is held by that air (CCRP 2024; Monteith 1981; Zhuang et al. 2021). As the temperature of the air rises, RH declines. For the Seashore, water deficits are projected in both hot-dry and warm-wet climate futures (Figure 20; CCRP 2024). The warm-wet future, which projects increased precipitation and shorter intervals between droughts, would be counteracted by evaporation into a warmer atmosphere (Behmanesh et al. 2015; CCRP 2024; Zhou et al. 2023). Because VPD is a function of both ambient temperature and RH, globally VPD is anticipated to increase with climate change (CCRP 2024, Corak et al. 2025; Novick et al. 2016).

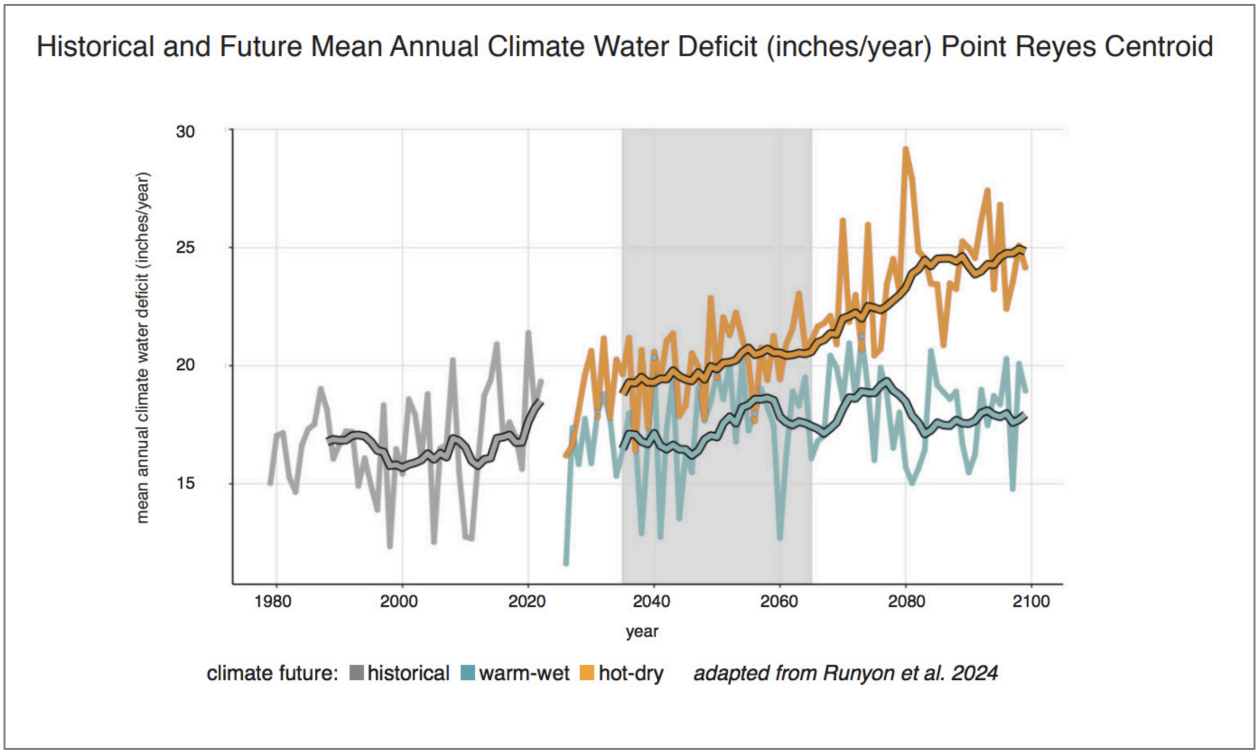

Figure 20. Comparison of observed climate water deficit at Point Reyes (inches/year) against park climate futures. In grey, historical trends, 1979–2022 for climate data sourced from Bear Valley (toward the interior of the park). The orange trend line highlights a hot-dry future, while the blue line highlights a warm-wet future. Smoothed lines represent 10-year running averages. Climatic water deficit indicates landscape aridity by quantifying the deficit of water available to plants by comparing potential ET against actual ET.

NPS / CCRP

VPD and Relative Humidity

Long-term trend data for Bodega Bay indicated that during what are typically the foggiest months of the year (June through August), VPD has declined since 1988 (Figure 6). Contrary to climate models, even as temperatures have warmed, there was a significant offset by historical trends in rising humidity along the coastline between June and August (Figure 7). Using observations of RH above 98% as a proxy for fog, we found a moderate year-round increase in low cloud/fog coverage for Bodega Bay (Appendix A; NOAA 2025). Because atmospheric moisture deficits drive evaporative demand, VPD is directly related to plant water use efficiency and hydraulic status (Grossiord et al. 2020; Schönbeck et al. 2022). Higher relative humidity mitigates moisture loss from these systems, and water resources may be provided by fog or low cloud coverage (Baldocchi et al. 2019). While there was no trend in VPD at Point Reyes, average summertime VPD values for both Point Reyes G Ranch and Bodega Bay fell below 0.20 kPa. A mean 0.16 kPa at G Ranch and a mean 0.07 kPa for Bodega Bay represent high saturation of atmospheric moisture and minimal to near-absent evaporative demand on plants during a period of the year when water resources are most limited (Grossiord et al. 2020). Climate water deficit—the difference between potential evapotranspiration and actual evapotranspiration—is projected to increase at the Seashore by 1.4 (warm-wet) to 4 (hot-dry) inches/per year, by 2050 (CCRP 2024). However, maritime influence of fog may offset extreme deficits by reducing evaporative demand. Further data that can directly measure incoming fog-water and fog and low cloud coverage will be imperative to explaining VPD trends and tracking long-term change in VPD at these coastal sites.

Wind Speed

There was no significant change in wind speed between 2007 and 2025 along the coast at either Bodega Bay or Point Reyes G Ranch by season or time of day (Tables 1 and 2). However, the data for Point Reyes G Ranch reveals unique seasonal relationships between wind speed, wind direction, and factors that have bearing on both water and energy balance. Through convection, wind is a vehicle for homogenizing meteorological conditions and for increasing the interface between physical and biological aspects of a landscape (such as soil or plant tissue) as well as meteorological conditions (Houghton and Cramer 1951; Wilson et al. 2002). The effects of wind are therefore directly associated with ambient conditions of temperature and humidity (Schymanski and Or 2015).

While wind speed at Point Reyes G Ranch had no correlation with ambient temperature during any month of the year, wind speed did correlate with RH during times of the year with the lowest precipitation (Table 1 and Figure 8). During summer seasonal drought, RH decreased with increasing wind speed, highlighting the role wind can play in affecting moisture gradients and exposing perennial plants to drought-related fatigue (Dixon and Grace 1984). June through August are the foggiest months of the year and also the months with the least precipitation (Goodman 1977). For these months, the negative relationship between wind speed and both RH and solar radiation may indicate fog dissipation (i.e., afternoon wind brings dry air into foggy sites). This may accelerate latent heat transfer through evaporation when wind was more intense (Bardoel et al. 2025; Dione et al. 2023; Tag 1979).

During the remainder of the year, including the rainy season, there was no correlation between wind speed and RH. This may be explained by high variability of entrained air into this system or negligible difference between entrained parcels of air (Geiger et al. 1995). In some winter months, low wind speeds were associated with low RH and may reflect interplay between wind and incoming storm systems and well-saturated soils. In other words, wind (a mixing force) may have a statistically significant effect on RH during most of the year, but not in a consistent direction. Only in the summer do we see consistency when it comes to coastal fog and wind patterns. Also, this mixing force is only discernable if the things being mixed (in this case parcels of air) are dissimilar enough that a mixed parcel is different than the original unmixed parcels.

Wind Direction

Both Bodega Bay and Point Reyes G Ranch indicated a significant increase in wind with a NW to N (315–360°) bearing over the duration of the observed years (Table 1 and Figure 9). While this trend occurred only between December and February at Bodega Bay, at Point Reyes G Ranch, this trend spanned March through November, with a most pronounced increase in 315–360° bearing winds during the summer. Winds with a 315–360° bearing have an established relationship with the formation of fog and low clouds along the California Coast (Torregrosa et al. 2015). Additionally, onshore movement of fog and low clouds correlates with coastlines that run perpendicular to these winds (Baldocchi et al. 2019; Torregrosa et al. 2015). Long-term increase in wind from this bearing during summer could potentially increase fog and low cloud coverage at Point Reyes during this period (Table 2). Variation between wind patterns and how wind was intercepted at these two weather monitoring sites is likely defined by distinct geography (Dorman et al. 2013; Torregrosa et al. 2015). Located on a peninsula, Point Reyes G Ranch lies approximately 10 miles from the edge of the North American continent, offering unobstructed exposure to North-South winds. By contrast, BML lies on a peninsula less than 2 miles from the continental landmass and does not directly intercept wind with a Northern bearing. Unlike Bodega Bay, where a low, wide valley known as the Petaluma Gap allows for East-West airflow, Point Reyes G Ranch is cut off from the interior by Inverness and Bolinas Ridges (Neiman et al. 2006).

While wind from the E and NE are infrequent along the Point Reyes coastline, these wind patterns during the fall in Northern and Central California are associated with the movement of hot, dry air masses known as the Diablo Winds, associated with promoting conditions favorable for wildfire (Liu et al. 2021). There was a statistically significant change, albeit weak, in the proportion of wind with an E or NE bearing for either Bodega Bay or Point Reyes G Ranch (Table 1) for two months—November and January. This weak change coincides with a period of October through March most associated with Diablo wind events (Smith et al. 2018). Though this increase in NE winds is subtle, the number of Diablo wind events per year in the San Francisco Bay Area has historically averaged 0.9–1.6 days, making the confluence of dry terrestrial conditions and dry, hot air an acute factor for exacerbating risk of wildfire as seen in the recent Atlas, Nuns, and Tubbs Fires (McClung and Mass 2020; Schmidt 2024).

During the rainy season there was a correlation between Point Reyes G Ranch wind direction and precipitation, with the strongest correlation between March and May (Figure 10). Total annual precipitation was greatest when the wind bearing was predominantly 240° (15° West of SW). Annual precipitation was lowest in years when the mean bearing was 280° (ten degrees North of due West). This trend is consistent with winter weather patterns along the Central Coast, where storm systems are largely driven by a wind with a 190° to 220° bearing (White et al. 2003).

Solar Radiation and Cloud Coverage

There was a consistent downward trend in total solar radiation for the duration that data were collected at Bodega Bay, 2009 to 2025 (Figure 11). Similarly, since 2019 (when DRI replaced the G Ranch photometer), there has been a significant decline in solar radiation at Point Reyes (Figure 12, Appendix A). While increased exposure to PAR can have positive effects on plant growth, energy balance through leaf traits and physiological response are required to offset NIR and mitigate heat stress. With latent heat-loss—a primary driver of leaf energy balance—reduced solar radiation through cloud-cover may improve water use efficiency by reducing energy balance requirements (Iacobellis and Cayan 2013; McCree 1971; Sridhar and Elliott 2002). Fog events can also greatly reduce evaporation through decreased VPD, as well as soil and leaf wetting (Fischer et al. 2009; Ritter et al. 2009). In a high drought-frequency scenario, illustrated in the hot-dry climate future, fog and low cloud moisture deposition may prove a critical supplement for plant life. Decline in solar radiation complements both soil temperatures declines and soil moisture increases over this same period (Table 1; Figure 17). These time series point to the relationship between these variables but were too abbreviated to establish any long-term trend at Point Reyes.

The relationship between wind and solar radiation indicated that during the summer months, wind may dissipate fog and low cloud cover and reduce associated high humidity. Solar radiation correlated positively with wind speed at both Bodega Bay and Point Reyes G Ranch (Figures 13 and 14). June through September is historically associated with reduced high-altitude cloud cover but increased low clouds and fog (Goodman 1977). Therefore, solar radiation data offer strong evidence for fog during these months. DRI at Point Reyes G Ranch measured wind speeds at a height of less than 5 meters above the ground. Therefore, the positive relationship between wind speed and solar radiation was a suitable proxy for the positive correlation between wind speed and low clouds and fog.

Soil Conditions

Between 2019 and 2025, average soil temperatures at Point Reyes declined, a trend accompanied by declining amplitude between soil temperature highs and lows (Figures 15 and 16). The duration of the Point Reyes dataset is insufficient to determine any historical trend in soil temperatures at Point Reyes G Ranch. However, this pattern paralleled both a decline in solar radiation at this site (a proxy for cloud and fog cover, Figure 12), as well as an increase in soil moisture content over this same time span (Table 1). The data were indicative of the interrelationship between soil temperature and soil moisture and low clouds and fog which influence water storage and evaporation. While surface soil temperatures were not recorded at this met station, we can expect long-term trends in cloud and fog coverage at Point Reyes to impact surface soil temperatures by insulating, buffering or scattering long-wave radiation in the summer (Miller 1997; Sui et al. 2008).

Because the tissue and meristems of many coastal grassland species grow in close proximity to the soil and experience the microclimatic effects of re-radiation, soil temperatures play a critical role in energy balance among dominant plant communities at Point Reyes (Horst and Nelson 1979). Understanding how cloud cover mediates leaf temperatures directly addresses the variable of evaporative transpiration that defines the climate water deficit described in park climate projections

(CCRP 2024; Baker and Myhre 1969). With a positive correlation between soil temperature and soil moisture at this site (Figure 17), we may anticipate increased tension on the water-column and latent heat loss (evaporative cooling) among coastal plants when there are warmer, drier soil conditions (Allen et al. 2015; Anderegg and Meinzer 2015; Volaire et al. 1998). Regardless of the uncertainty of future precipitation, cooler summertime soil temperatures mediated by fog and low cloud cover at coastal Point Reyes would provide some offset to seasonal drought stress among perennial plants anticipated in both warm-wet and hot-dry climate futures (Figure 3; CCRP 2024; Kolb and Robberecht 1996; Davis and Sherman 1992).

Conclusion

Historical data for the Point Reyes coastline were consistent with both global and climate change trends and projection insofar as temperature was concerned. Historical warming at Point Reyes fell within projected values for both warm and hot futures. Both sites also observed an increase in 99^{th} percentile heat events. While there was no long-term change in annual precipitation, increasing climate water deficit has been anticipated as a most likely outcome under both warm-wet and hot-dry futures as increasing global temperatures drive increasing evaporative demand. Here, 37 years of data collected at Bodega Bay illustrated an increase in RH and decline in VPD over this period. Regression analysis between climate factors highlights the important role that summertime low clouds and fog may play in reducing VPD in areas influenced by maritime climate. These low cloud and fog events may serve to offset soil warming and ambient temperature increases. Low clouds and fog could also reduce moisture loss from this system during critical times of the year and act as a buffer to extended drought anticipated in the hot-dry projection. Alternatively, the relationship between wind speed and these variables indicated the important role of convection in counteracting the effects of low cloud and fog or in determining the types of weather intercepted at Point Reyes. Refining our understanding of the interrelationships and trajectories of these climate conditions will benefit from continued monitoring of climate variables at Point Reyes, as well as more specific data collection for fog and low cloud coverage events and associated moisture inputs into this system. Additionally, future data that can include surface soil temperature will provide important information into the effects of fog and cloud coverage in limiting potential thermal stress experienced by grasses and forbs native to the Point Reyes Peninsula.

Literature Cited

Albano, C.M., M.D. Dettinger, and A. Harpold. 2020. Patterns and drivers of atmospheric river precipitation and hydrologic impacts across the western United States. Journal of Hydrometeorology 21: 143−159. https://doi.org/10.1175/JHM-D-19-0119.1

Alizadeh, O. 2022. Advances and Challenges in Climate Modeling. Climatic Change 170(18). https://doi.org/10.1007/s10584-021-03298-4

Allen, C.D., D.D. Breshears, and N.G. McDowell. 2015. On Underestimation of Global Vulnerability to Tree Mortality and Forest Die-off from Hotter Drought in the Anthropocene. Ecosphere 6(8): art129. https://doi.org/10.1890/ES15-00203.1

Anderegg, W.R.L., and F.C. Meinzer. 2015. Wood Anatomy and Plant Hydraulics in a Changing Climate. Pages 235–253 *in* U. Hacke, Ed. Functional and Ecological Xylem Anatomy. Springer International Publishing, Switzerland. https://doi.org/10.1007/978-3-319-15783-2_9

Aylor, D.E., J-Y. Parlange, and A.D. Krikorian. 1973. Stomatal Mechanics. American Journal of Botany 60: 163–171. https://doi.org/10.1002/j.1537-2197.1973.tb10213.x

Baker, D.N., and D.L. Myhre. 1969. Effects of Leaf Shape and Boundary Layer Thickness on Photosynthesis in Cotton (Gossypium hirsutum). Physiologia Plantarum 22(5): 1043–1049. https://doi.org/10.1111/j.1399-3054.1969.tb07463.x

Baldocchi, D., D. Dralle, C. Jiang, and Y. Ryu. 2019. How Much Water Is Evaporated Across California? A Multiyear Assessment Using a Biophysical Model Forced With Satellite Remote Sensing Data. Water Resources Research 55(4): 2722–2741. https://doi.org/10.1029/2018WR023884

Bardoel, S.L., S. Hoch, J. Ruiz-Plancarte, L. Lenain, I. Gultepe, A.A. Grachev, S. Gaberšek, Q. Wang, and H.J.S. Fernando. 2025. Study of Fog Dissipation in an Internal Boundary Layer on Sable Island. Quarterly Journal of the Royal Meteorological Society 151(766): e4891. https://doi.org/10.1002/qj.4891

Behmanesh, J., N. Azad Talatappeh, M. Montaseri, H. Rezayi, and K. Khalili. 2015. Climate Change Impact on Reference Evapotranspiration, Precipitation Deficit and Vapor Pressure Deficit in Urmia. Water and Soil Science 25(2): 79–91. https://water-soil.tabrizu.ac.ir/article_3894_en.html

Clemesha, R.E.S., K. Guirguis, A. Gershunov, I.J. Small, and A. Tardy. 2017. California Heat Waves: Their Spatial Evolution, Variation, and Coastal Modulation by Low Clouds. Climate Dynamics 50(11): 4285–4301. https://doi.org/10.1007/s00382-017-3875-7

Climate Change Response Program (CCRP). 2024. Point Reyes National Seashore Climate Futures Summary. National Park Service. Fort Collins, Colorado. https://irma.nps.gov/DataStore/DownloadFile/705860

Corak, N.K., P.E. Thornton, and L.E.L. Lowman. 2025. A High Resolution, Gridded Product for Vapor Pressure Deficit Using Daymet. Scientific Data 12(1): 256. https://doi.org/10.1038/s41597-025-04544-5

Cordeira, J.M., J. Stock, M.D. Dettinger, A.M. Young, J.F. Kalansky, and F.M. Ralph. 2019. A 142-Year Climatology of Northern California Landslides and Atmospheric Rivers. Bulletin of the American Meteorological Society 100: 1499–1509. https://doi.org/10.1175/BAMS-D-18-0158.1

Davis, L.H., and R.J. Sherman. 1992. Ecological Study of the Rare Chorizanthe Valida (Polygonaceae) at Point Reyes National Seashore, California. Madroño 39(4): 271–280. https://www.jstor.org/stable/41424922

Desert Research Institute (DRI). 2025. Projects and Collaborations. Desert Research Institute website. https://www.dri.edu/projects/ (accessed September 5, 2025).

Dione, C., M. Haeffelin, F. Burnet, C. Lac, G. Canut, J. Delanoë, J-C. Dupont, et al. 2023. Role of Thermodynamic and Turbulence Processes on the Fog Life Cycle during SOFOG3D Experiment. Atmospheric Chemistry and Physics 23(24): 15711–15731. https://doi.org/10.5194/acp-23-15711-2023

Dixon, M., and J. Grace. 1984. Effect of Wind on the Transpiration of Young Trees. Annals of Botany 53(6): 811–819. https://doi.org/10.1093/oxfordjournals.aob.a086751

Dorman, C.E., J.F. Mejia, and D. Koračin. 2013. Impact of U.S. west coastline inhomogeneity and synoptic forcing on winds, wind stress, and wind stress curl during upwelling season. Journal of Geophysical Research: Oceans 118(9): 4036–4051. https://doi.org/10.1002/jgrc.20282

Ehleringer, J.R., and O. Björkman. 1978. A Comparison of Photosynthetic Characteristics of Encelia Species Possessing Glabrous and Pubescent Leaves. Plant Physiology 62(2): 185–190. https://doi.org/10.1104/pp.62.2.185

Evens, J. 2008. Natural History of the Point Reyes Peninsula: Fully Revised and Expanded Edition. University of California Press, Berkeley, California.

Finnigan, J.J. 2021. The Turbulent Wind in Plant and Forest Canopies. Pages 17–63 *in* Plant Disturbance Ecology, second edition, Edward A. Johnson and Kiyoko Miyanishi, editors. Academic Press, San Diego, California. https://doi.org/10.1016/B978-0-12-818813-2.00002-2

Fischer, D.T., C.J. Still, and A.P. Williams. 2009. Significance of Summer Fog and Overcast for Drought Stress and Ecological Functioning of Coastal California Endemic Plant Species. Journal of Biogeography 36(4): 783–99. https://doi.org/10.1111/j.1365-2699.2008.02025.x

García-Reyes, M., and J.L. Largier. 2012. Seasonality of Coastal Upwelling off Central and Northern California: New Insights, Including Temporal and Spatial Variability. Journal of Geophysical Research: Oceans 117(C3). https://doi.org/10.1029/2011JC007629

Geiger, R., R.H. Aron, and P. Todhunter. 1995. The Climate Near the Ground. Wiesbaden: Vieweg+Teubner Verlag. https://doi.org/10.1007/978-3-322-86582-3

Geophysical Fluid Dynamics Laboratory (GFDL). 2025. Climate Modeling – Geophysical Fluid Dynamics Laboratory. NOAA. https://www.gfdl.noaa.gov/climate-modeling/ (accessed September 5, 2025).

Gomez, M.S., J. Lundquist, J. Mirocha, and R. Arthur. 2023. Investigating the Physical Mechanisms that Modify Wind Plant Blockage in Stable Boundary Layers. Wind Energy Science 8(7): 1049–1069. https://doi.org/10.5194/wes-8-1049-2023

Goodman, J. 1977. The Microstructure of California Coastal Fog and Stratus. Journal of Applied Meteorology 16(10): 1056–1067. https://doi.org/10.1175/1520-0450(1977)016%3C1056:TMOCCF%3E2.0.CO;2

Grossiord, C., T.N. Buckley, L.A. Cernusak, K.A. Novick, B. Poulter, R.T.W. Siegwolf, J.S. Sperry, and N.G. McDowell. 2020. Plant Responses to Rising Vapor Pressure Deficit. New Phytologist 226(6): 1550–1566. https://doi.org/10.1111/nph.16485

Hall, A., S. Rahimi, J. Norris, N. Ban, N. Siler, L.R. Leung, P. Ullrich, K.A. Reed, A.F. Prein, and Y. Qian. 2024. An Evaluation of Dynamical Downscaling Methods Used to Project Regional Climate Change. Journal of Geophysical Research: Atmospheres 129(24): e2023JD040591. https://doi.org/10.1029/2023JD040591

Horst, G.L., and C.J. Nelson. 1979. Compensatory Growth of Tall Fescue Following Drought. Agronomy Journal 71(4): 559–563. https://doi.org/10.2134/agronj1979.00021962007100040010x

Houghton, H.G., and H.E. Cramer. 1951. A Theory of Entrainment in Convective Currents. Journal of the Atmospheric Sciences 8: 95–102. https://doi.org/10.1175/1520-0469(1951)008%3C0095:ATOEIC%3E2.0.CO;2

Iacobellis, S.F., and D.R. Cayan. 2013. The Variability of California Summertime Marine Stratus: Impacts on Surface Air Temperatures. Journal of Geophysical Research: Atmospheres 118(16): 9105–9122. https://doi.org/10.1002/jgrd.50652

Inada, K. 1976. Action Spectra for Photosynthesis in Higher Plants. Plant and Cell Physiology 17(2): 355–365. https://doi.org/10.1093/oxfordjournals.pcp.a075288

Ingraham, N.L., and R.A. Matthews. 1995. The Importance of Fog-Drip Water to Vegetation: Point Reyes Peninsula, California. Journal of Hydrology 164(1): 269–285. https://doi.org/10.1016/0022-1694(94)02538-M

John, A., J.D. Olden, M.F. Oldfather, M.M. Kling, and D.D. Ackerly. 2024. Topography Influences Diurnal and Seasonal Microclimate Fluctuations in Hilly Terrain Environments of Coastal California. PLOS ONE 19(3): e0300378. https://doi.org/10.1371/journal.pone.0300378

Jones, H.G. 2013. Plants and Microclimate: A Quantitative Approach to Environmental Plant Physiology, third edition. Cambridge University Press, Cambridge. https://doi.org/10.1017/CBO9780511845727

Kolb, P.F., and R. Robberecht. 1996. High Temperature and Drought Stress Effects on Survival of Pinus Ponderosa Seedlings. Tree Physiology 16(8): 665–672. https://doi.org/10.1093/treephys/16.8.665

Kulkarni, S., M.C. Deo, and S. Ghosh. 2019. Performance of the CORDEX Regional Climate Models in Simulating Offshore Wind and Wind Potential. Theoretical and Applied Climatology 135(3): 1449–1464. https://doi.org/10.1007/s00704-018-2401-0

Lambers, H., F.S. Chapin, and T.L. Pons. 1998. Plant Physiological Ecology. Springer, New York, New York. https://doi.org/10.1007/978-1-4757-2855-2

Liu, Y-C., P. Di, S-H. Chen, X. Chen, J. Fan, J. DaMassa, and J. Avise. 2021. Climatology of Diablo Winds in Northern California and Their Relationships with Large-Scale Climate Variabilities. Climate Dynamics 56(3): 1335–1356. https://doi.org/10.1007/s00382-020-05535-5

McClung, B., and C.F. Mass. 2020. The Strong, Dry Winds of Central and Northern California: Climatology and Synoptic Evolution. Weather and Forecasting 35(5): 2163–2178. https://doi.org/10.1175/WAF-D-19-0221.1

McCree, K.J. 1971. The Action Spectrum, Absorptance and Quantum Yield of Photosynthesis in Crop Plants. Agricultural Meteorology 9: 191–216. https://doi.org/10.1016/0002-1571(71)90022-7

McSweeney, R. 2018. Q&A: How Do Climate Models Work? Carbon Brief website. https://www.carbonbrief.org/qa-how-do-climate-models-work/

Miller, R.L. 1997. Tropical Thermostats and Low Cloud Cover. Journal of Climate 10(3): 409–440. https://doi.org/10.1175/1520-0442(1997)010%3C0409:TTALCC%3E2.0.CO;2

Monteith, J.L. 1981. Evaporation and Surface Temperature. Quarterly Journal of the Royal Meteorological Society 107(451): 1–27. https://doi.org/10.1002/qj.49710745102

National Oceanic and Atmospheric Administration (NOAA). 2025. Discussion on Humidity. National Weather Service website. https://www.weather.gov/lmk/humidity (accessed September 5, 2025).

National Park Service (NPS). 2024. Point Reyes National Seashore: Weather. NPS website. https://www.nps.gov/pore/learn/nature/weather.htm

National Park Service (NPS). 2025. Point Reyes National Seashore. NPS website. https://www.nps.gov/pore/index.htm

Neiman, P.J., F.M. Ralph, A.B. White, D.D. Parrish, J.S. Holloway, and D.L. Bartels. 2006. A Multiwinter Analysis of Channeled Flow through a Prominent Gap along the Northern California Coast during CALJET and PACJET. Monthly Weather Review 134: 1815–1841. https://doi.org/10.1175/MWR3148.1

Novick, K.A., D.L. Ficklin, P.C. Stoy, C.A. Williams, G. Bohrer, A.C. Oishi, S.A. Papuga, et al. 2016. The Increasing Importance of Atmospheric Demand for Ecosystem Water and Carbon Fluxes. Nature Climate Change 6(11): 1023–27. https://doi.org/10.1038/nclimate3114

Pielke, R.A., Sr., and R.L. Wilby. 2012. Regional Climate Downscaling: What's the Point? Eos, Transactions American Geophysical Union 93(5): 52–53. https://doi.org/10.1029/2012EO050008

Pierce, D.W., and D.R. Cayan. 2016. Downscaling Humidity with Localized Constructed Analogs (LOCA) over the Conterminous United States. Climate Dynamics 47(1): 411–431. https://doi.org/10.1007/s00382-015-2845-1

Pierce, D.W., D.R. Cayan, and B.L. Thrasher. 2014. Statistical Downscaling Using Localized Constructed Analogs (LOCA). Journal of Hydrometeorology 15(6): 2558–2585. https://doi.org/10.1175/JHM-D-14-0082.1

Ritter, A., C.M. Regalado, and G. Aschan. 2009. Fog Reduces Transpiration in Tree Species of the Canarian Relict Heath-Laurel Cloud Forest (Garajonay National Park, Spain). Tree Physiology 29(4): 517–528. https://doi.org/10.1093/treephys/tpn043

Ryan, A., and L. Parsons. 2011. Sonoma Spineflower (*Chorizanthe valida*) TE018180-4. Annual Report. U.S. Fish and Wildlife Service.

Runyon, A., J. Gross, G. Schuurman, D. Lawrence, and J. Reynolds. 2024. Methods for Assessing Climate Change Exposure for National Park Planning. National Park Service. https://doi.org/10.36967/2302720

Schmidt, J. 2024. County Wildfire Risk Ratings in Northern California: FAIR Plan Insurance Policies and Simulation Models vs. Red Flag Warnings and Diablo Winds. MPRA Paper No. 120195. Munich Personal RePEc Archive. https://mpra.ub.uni-muenchen.de/120195/

Schönbeck, L.C., P. Schuler, M.M. Lehmann, E. Mas, L. Mekarni, A.L. Pivovaroff, P. Turberg, and C. Grossiord. 2022. Increasing Temperature and Vapour Pressure Deficit Lead to Hydraulic Damages in the Absence of Soil Drought. Plant, Cell & Environment 45(11): 3275–3289. https://doi.org/10.1111/pce.14425

Schymanski, S.J., and D. Or. 2015. Wind Effects on Leaf Transpiration Challenge the Concept of "Potential Evaporation". *In* Proceedings of the International Association of Hydrological Sciences 371:99–107. https://doi.org/10.5194/piahs-371-99-2015

Schymanski, S.J., D. Breitenstein, and D. Or. 2017. Technical Note: An Experimental Set-up to Measure Latent and Sensible Heat Fluxes from (Artificial) Plant Leaves. Hydrology and Earth System Sciences 21(7): 3377–3400. https://doi.org/10.5194/hess-21-3377-2017

Smith, C., B.J. Hatchett, and M. Kaplan. 2018. A Surface Observation Based Climatology of Diablo-Like Winds in California's Wine Country and Western Sierra Nevada. Fire 1(2): 25. https://doi.org/10.3390/fire1020025

Sridhar, V., and R.L. Elliott. 2002. On the Development of a Simple Downwelling Longwave Radiation Scheme. Agricultural and Forest Meteorology 112(3): 237–243. https://doi.org/10.1016/S0168-1923(02)00129-6

Steeneveld, G.J., R.J. Ronda, and A.A.M. Holtslag. 2014. The Challenge of Forecasting the Onset and Development of Radiation Fog Using Mesoscale Atmospheric Models. Boundary-Layer Meteorology 154(2): 265–289. https://doi.org/10.1007/s10546-014-9973-8

Sui, C.-H., X. Li, C.-H. Ho, and K.-M. Lau. 2008. Effects of Radiative Cooling on the Tropical Convective Response to Sea Surface Temperature: 2-D Large Domain Cumulus Ensemble Simulations. Journal of Geophysical Research: Atmospheres 113(D8). https://doi.org/10.1029/2007JD008557

Tag, P.M. 1979. A Numerical Simulation of Fog Dissipation Using Passive Burner Lines. Part II: Sensitivity Experiments. Journal of Applied Meteorology and Climatology 18(11): 1455–1471. https://doi.org/10.1175/1520-0450(1979)018%3C1455:ANSOFD%3E2.0.CO;2

Torregrosa, A., C. Combs, and J. Peters. 2015. GOES-derived fog and low cloud indices in north and central California ecological analyses. Earth and Space Science 3(2): 46−67. https://agupubs.onlinelibrary.wiley.com/doi/full/10.1002/2015EA000119

University of California, Davis (UCD). n.d. Coastal and Marine Sciences Institute, Bodega Marine Laboratory website. University of California, Davis. https://marinescience.ucdavis.edu/bml/about

Volaire, F., H. Thomas, N. Bertagne, E. Bourgeois, M-F. Gautier, and F. Lelièvre. 1998. Survival and Recovery of Perennial Forage Grasses under Prolonged Mediterranean Drought: II. Water Status, Solute Accumulation, Abscisic Acid Concentration and Accumulation of Dehydrin Transcripts in Bases of Immature Leaves. The New Phytologist 140(3): 451–460. https://doi.org/10.1046/j.1469-8137.1998.00287.x

Wang, Y., J.S. Sperry, W.R.L. Anderegg, M.D. Venturas, and A.T. Trugman. 2020. A Theoretical and Empirical Assessment of Stomatal Optimization Modeling. New Phytologist 227(2): 311–325. https://doi.org/10.1111/nph.16572

White, A.B., P.J. Neiman, F.M. Ralph, D.E. Kingsmill, and P.O.G. Persson. 2003. Coastal Orographic Rainfall Processes Observed by Radar during the California Land-Falling Jets Experiment. Journal of Hydrometeorology 4(2): 264–282. https://doi.org/10.1175/1525-7541(2003)4%3C264:CORPOB%3E2.0.CO;2

Wilson, K.B., D.D. Baldocchi, M. Aubinet, P. Berbigier, C. Bernhofer, H. Dolman, E. Falge, et al. 2002. Energy Partitioning between Latent and Sensible Heat Flux during the Warm Season at FLUXNET Sites. Water Resources Research 38(12): 1−30. https://doi.org/10.1029/2001WR000989

Winsberg, E. 2012. Values and Uncertainties in the Predictions of Global Climate Models. Kennedy Institute of Ethics Journal 22(2): 111–137. https://muse.jhu.edu/pub/1/article/484359

Zhou, X., Y. Cheng, L. Liu, Y. Huang, and H. Sun. 2023. Significant Increase in Water Vapor Pressure Correspond with Climate Warming Globally. Water 15(18): 3219. https://doi.org/10.3390/w15183219

Zhuang, Y., R. Fu, B.D. Santer, R.E. Dickinson, and A. Hall. 2021. Quantifying Contributions of Natural Variability and Anthropogenic Forcings on Increased Fire Weather Risk over the Western United States. Proceedings of the National Academy of Sciences 118(45): e2111875118. https://doi.org/10.1073/pnas.2111875118

Appendix A. Analyses Describing Diurnal, Seasonal, and Interannual Variability in Key Meteorological Drivers at Bodega Bay and Point Reyes G Ranch

Figures 21–28 present a set of complementary analyses describing diurnal, seasonal, and interannual variability in key meteorological drivers at Bodega Bay and Point Reyes G Ranch, including wind speed and direction, temperature extremes, humidity, and precipitation, as well as long-term trends and statistical relationships in these variables.

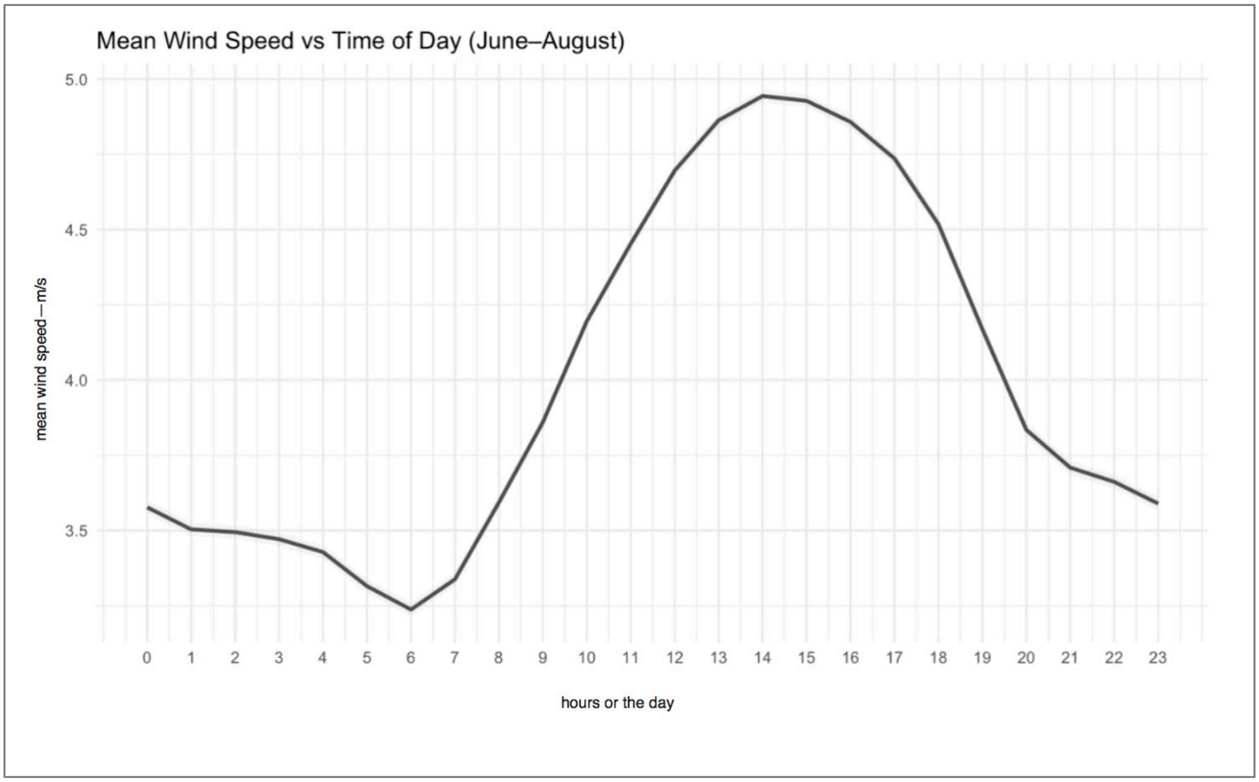

Figure 21. Mean wind speed vs. time of day, June–August. The figure illustrates how wind speed tracks a consistent pattern throughout the day. RH, air temperatures and solar radiation closely mirror this pattern. *NPS / GREGORY ARENA*

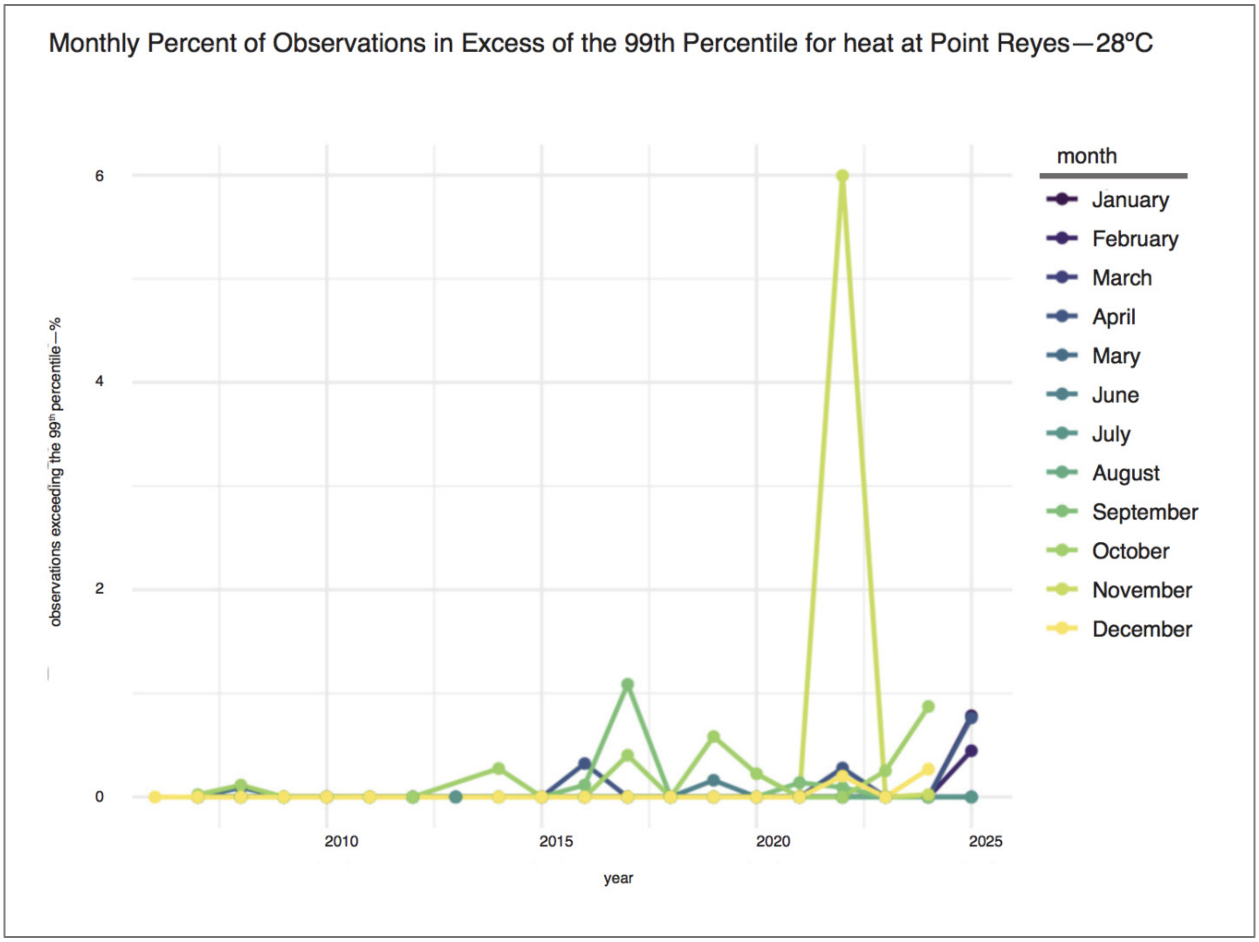

Figure 22. Monthly percentage of observations in excess of the 99th percentile for heat at Point Reyes. 99th percentile heat events are plotted as a percentage of total observations per month to account for data irregularities and gaps.

NPS / GREGORY ARENA

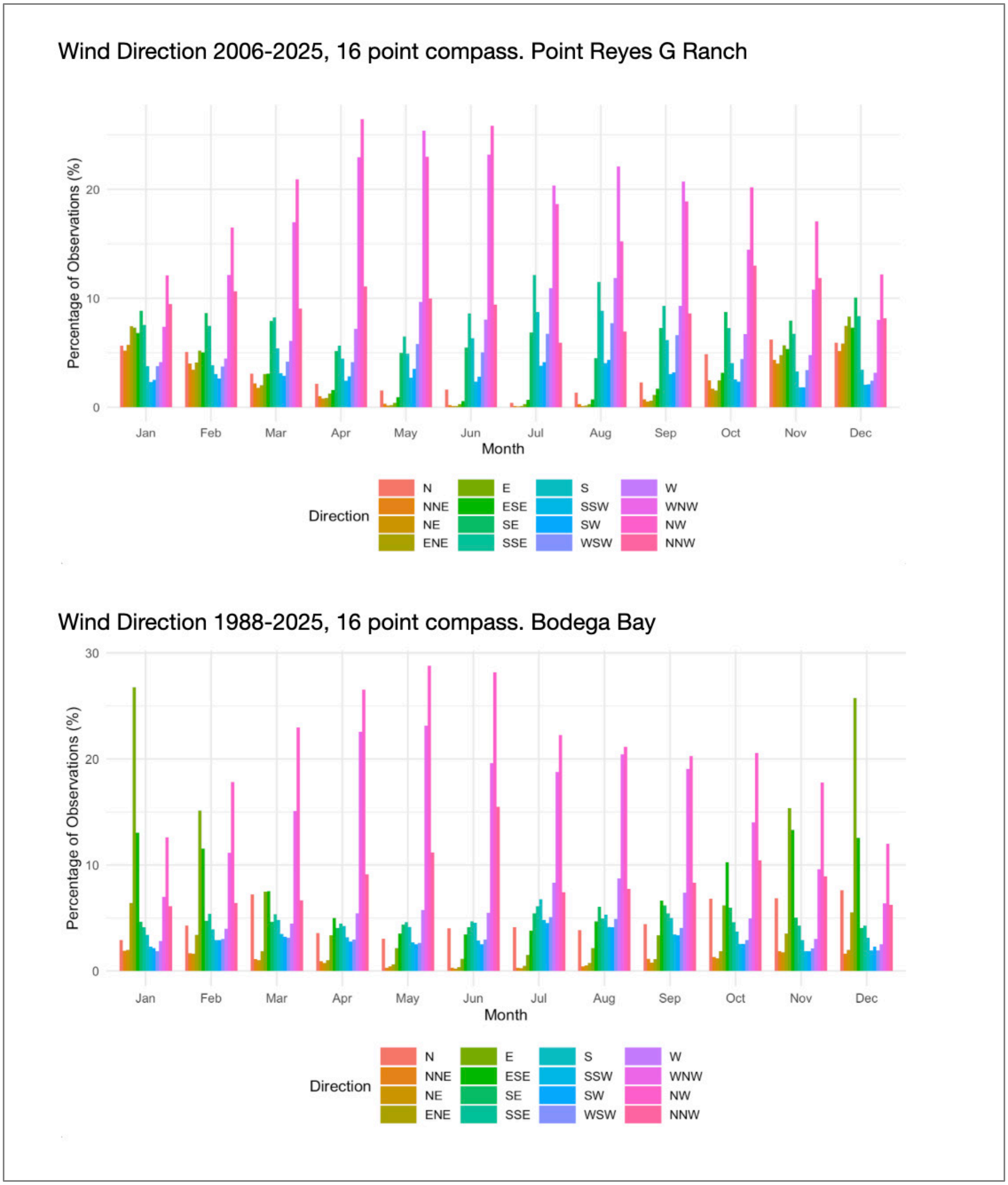

Figure 23. Wind direction 2006–2025, 16-point compass, Point Reyes G Ranch; and wind direction 1988–2025, 16-point compass, Bodega Bay. The average distribution of wind direction for each month is based on the percentage of observations recorded for each of the 16 compass subdivisions.

NPS / GREGORY ARENA

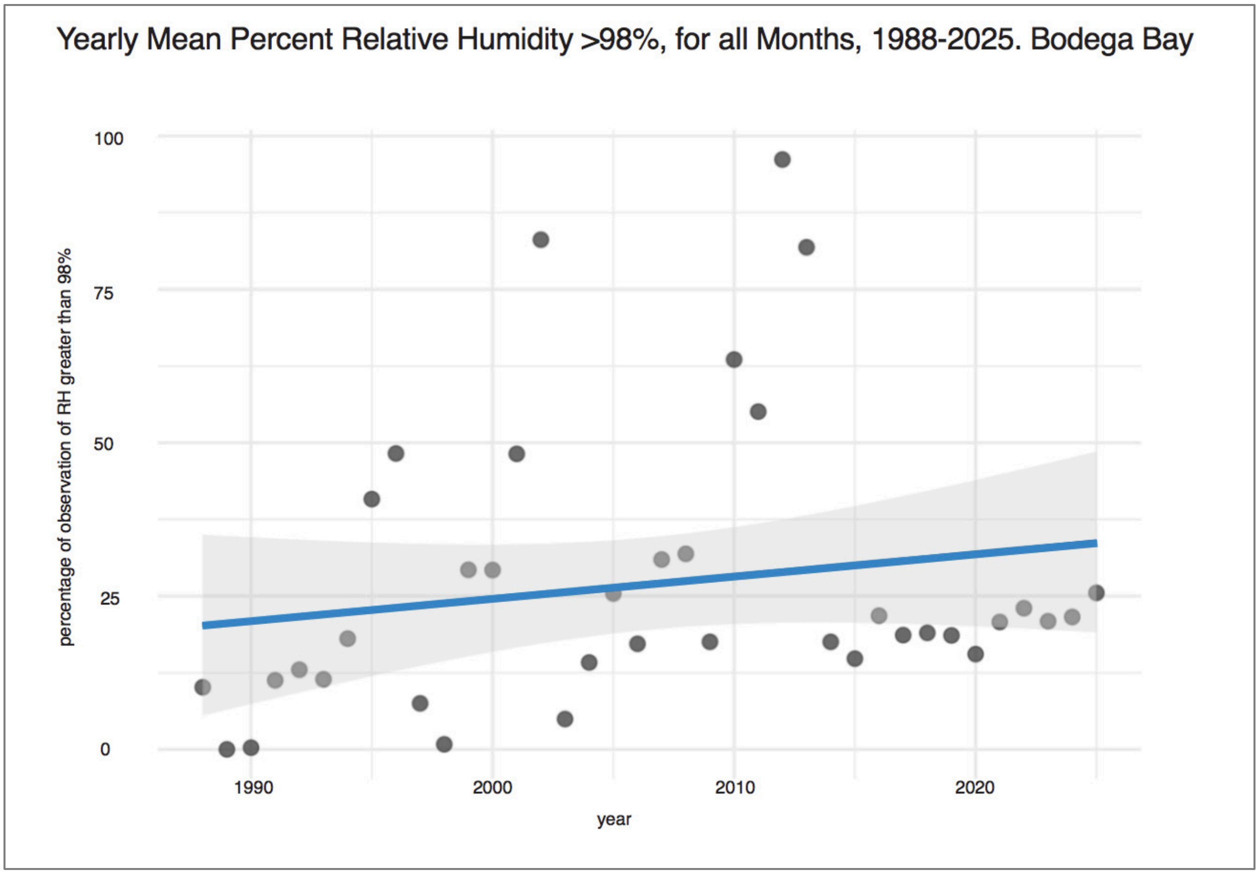

Figure 24. Yearly mean percent relative humidity greater than 98% for all months, Bodega Bay. Percent > 98% RH = −708.09 + 0.3664 × year, R^2 = 0.0317, F(1,36) = 1.1796, p = 0.2846, Mann–Kendall test: tau = 0.2648, p = 0.02002, Sen's slope estimate = 0.3592% per year.

NPS / GREGORY ARENA

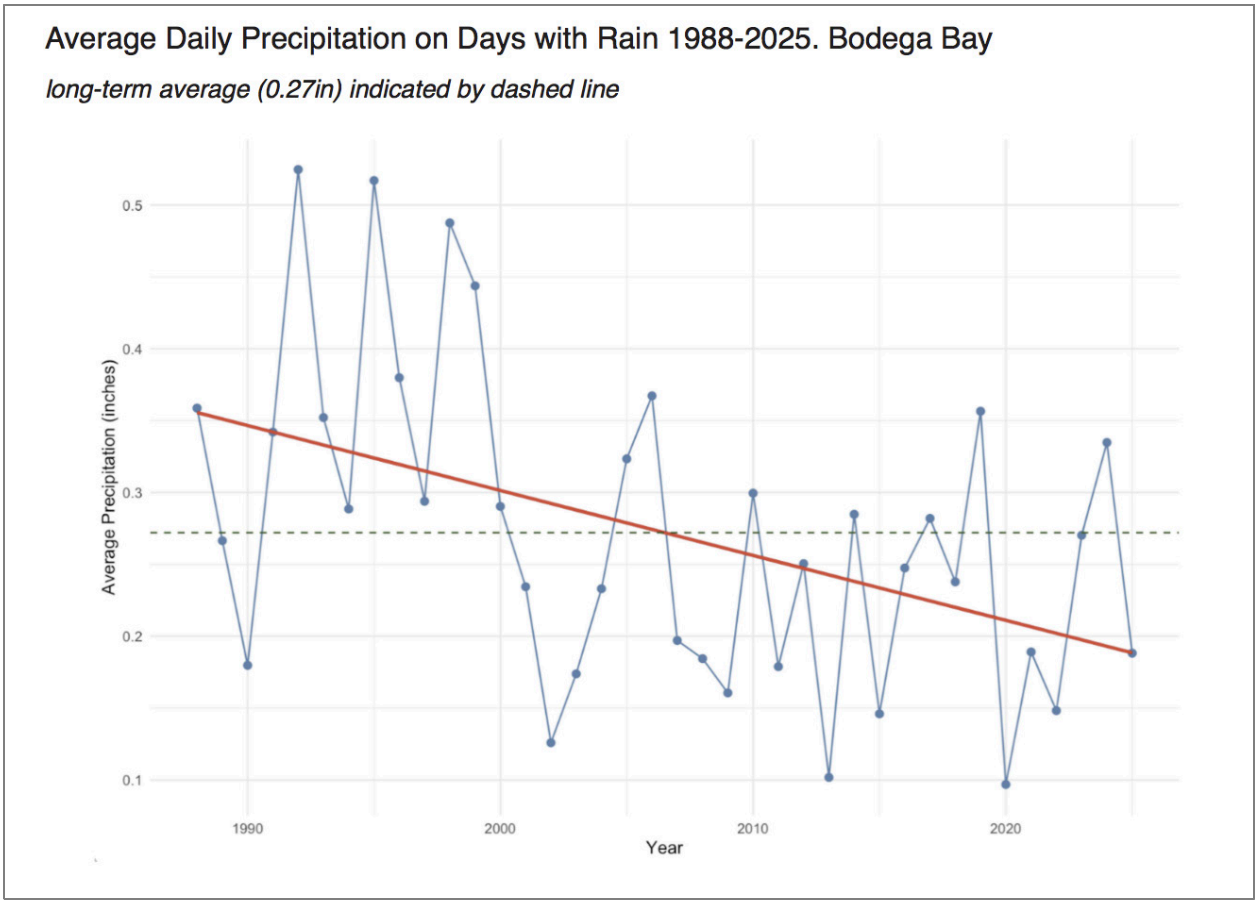

Figure 25. Average daily precipitation on days with rain at Bodega Bay, 1988–2025. $R^2 = 0.26$, $F(1,18) = 6.402$, $p = 0.021$, Mann–Kendall test: tau = 0.49, $p = 0.004$, regression slope = −23.076 + 0.0115 × year. *NPS / GREGORY ARENA*

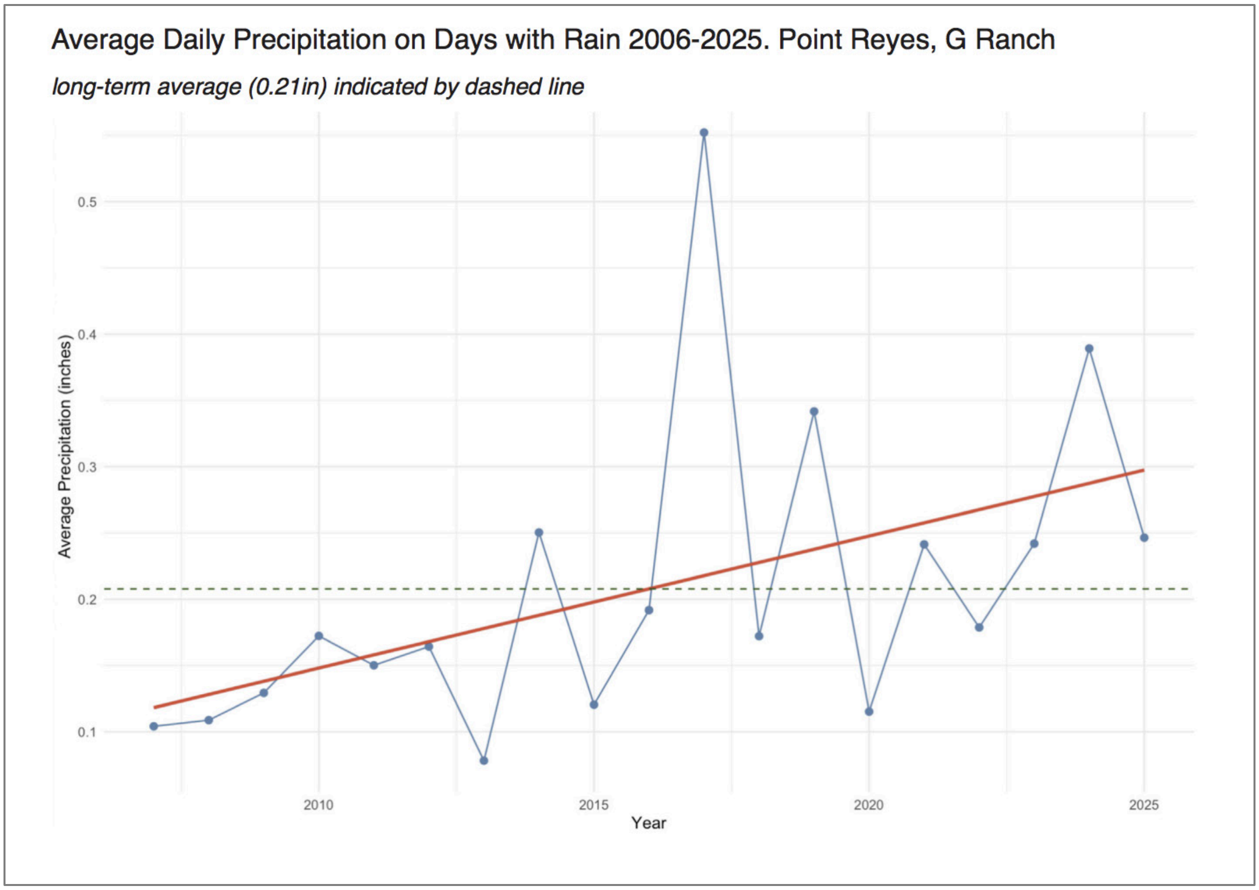

Figure 26. Average daily precipitation on days with rain, 2006–2025, Point Reyes G Ranch. $R^2 = 0.23$, $F(1,17) = 5.14$, $p = 0.037$, Mann–Kendall test: tau = 0.32, $p = 0.58$. Includes only days with measurable precipitation. Long-term average 0.21 inches indicated by dashed line.

NPS / GREGORY ARENA

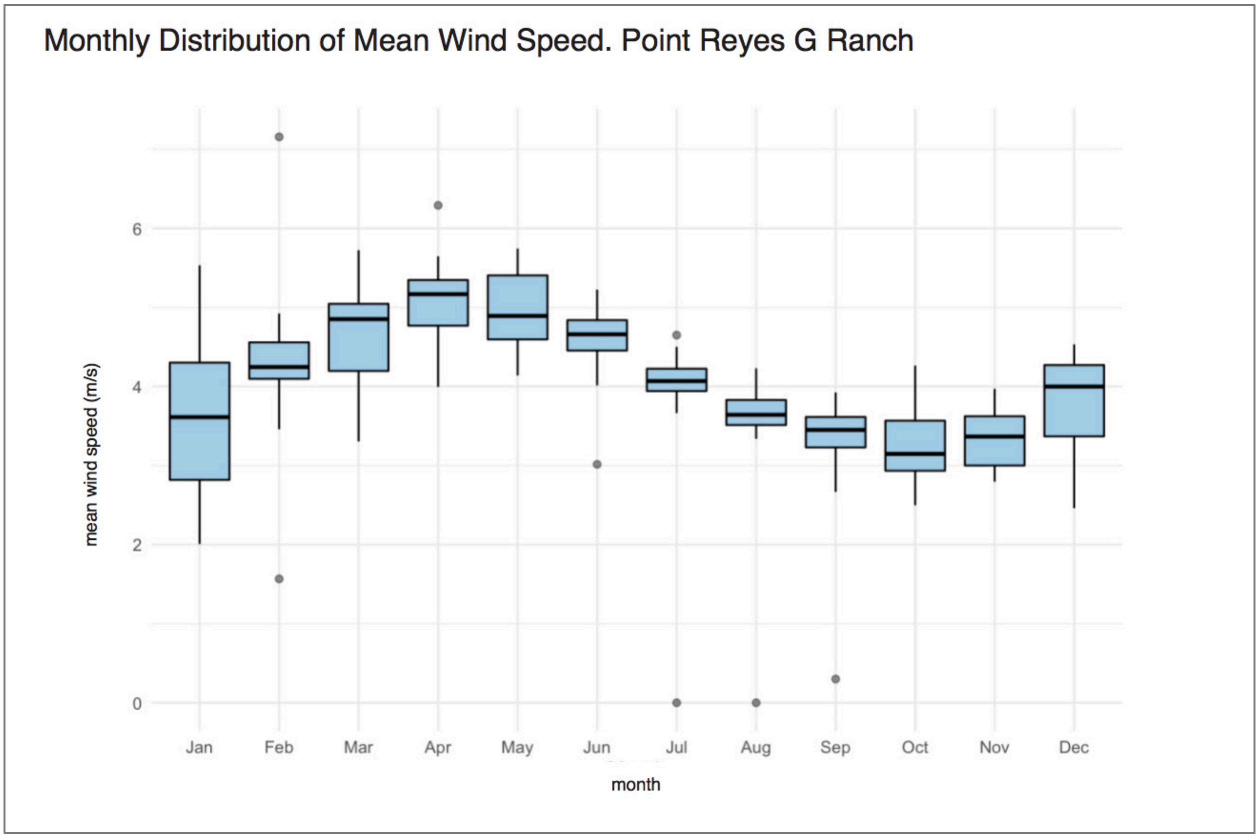

Figure 27. Monthly distribution of mean wind speed, Point Reyes G Ranch. Two-way ANOVA; $F(1,196) = 14.9$, $p < 0.000001$. Each box represents interannual variability within each month between 2006 and 2025. Highest average wind speeds at Point Reyes occur in April, May, June, and July at 4.67, 5.07, 4.95 and 4.57 m/s respectively.

NPS / GREGORY ARENA

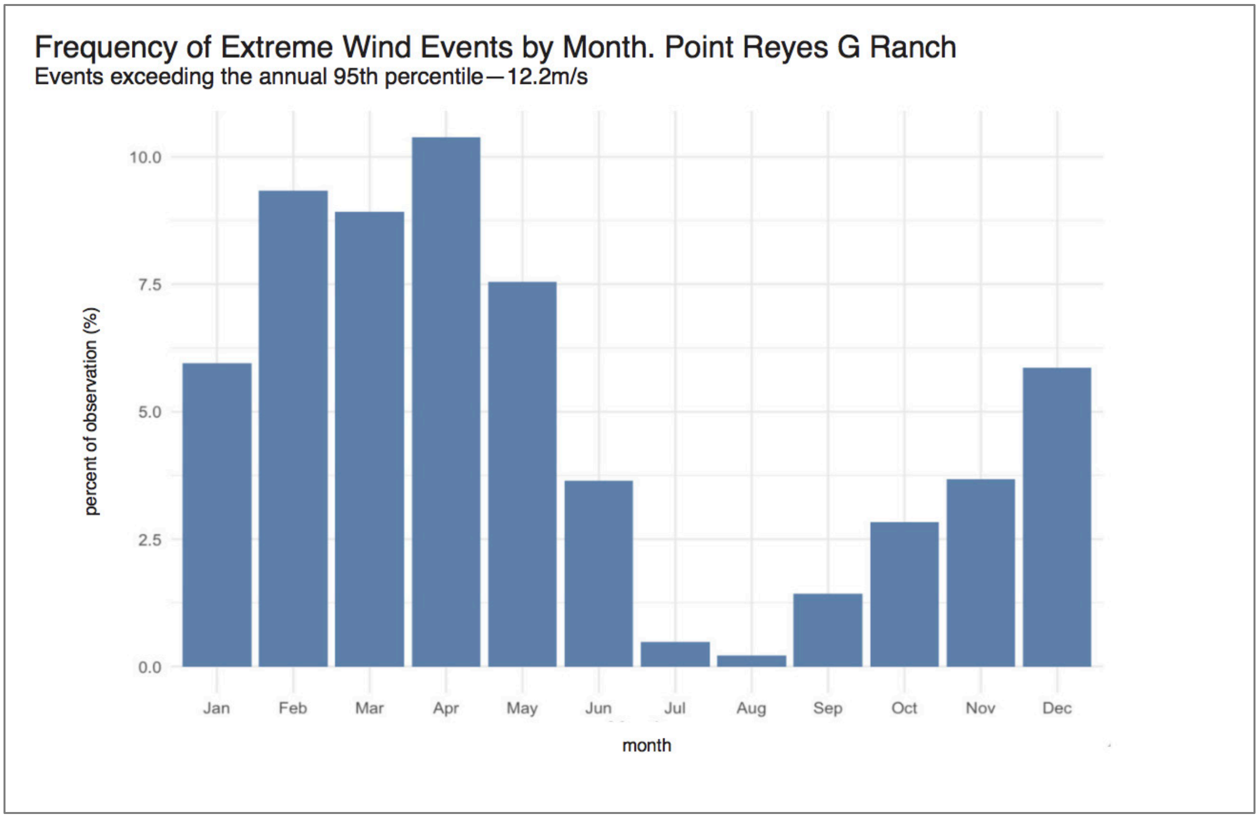

Figure 28. Frequency of extreme wind events by month, Point Reyes G Ranch. The figure shows events exceeding the annual 95th percentile wind speed threshold of 9.39 m/s.

NPS / GREGORY ARENA

Appendix B. Expanded Information About the Maintenance and Upkeep of the DRI Meteorological Station at Point Reyes G Ranch

Greg McCurdy, a research scientist and climatologist with DRI, was the primary point of contact for the Point Reyes G Ranch station at the time of writing. He oversees data QA/QC and station maintenance and was able to provide information on some of the anomalies observed in the data. McCurdy has maintained this station since 2006. Instrumentation has typically been replaced every 5–7 years, or based on sensor longevity, exposure, and unexpected events. The wind sensor has been replaced three times, the AT/RH sensor twice, and the rain gauge four times since 2006. The instrument enclosures (containing the main electronics and batteries) and the main tower were replaced once in 2017. There has been no replacement of soil moisture or soil temperature probe sensors since installation in 2020 and 2021. McCurdy services the station every 6–12 months. Visits are also scheduled when McCurdy or his team identify that a sensor is down or malfunctioning, which explains occasional gaps or interruptions in the data over one- to two-month periods. Notable breaks in these data trends that are explained by sensor replacements include solar radiation data for 2019. Scattered AT/RH data between 2012 and 2014 were the result of faulty batteries. Batteries were replaced in the winter of 2013 and 2014 for these sensors, but these sensors were neither moved, nor replaced during this time.

Regional meteorological climate anomalies are also evident in the data at both Point Reyes G Ranch and Bodega Marine Laboratory that do not reflect sensor error or calibration issues. These anomalies include a particularly warm year for the Bay Area in 2015 and 2020. The impacts of intense multi-year drought between 2011 and 2016 in California are also evident in these data. This multi-year drought was connected to the North Pacific High anticyclone (a seasonal phenomenon) which blocks incoming storm systems. These anticyclones exert a strong influence on continent and nearshore warming producing coastal summertime fog in the SF Bay Area and Northern California.

National Park Service
U.S. Department of the Interior

Science Report NPS/SR—2026/460
https://doi.org/10.36967/2318166

Natural Resource Stewardship and Science
1201 Oakridge Drive, Suite 150
Fort Collins, CO 80525

NPS 612/199752, July 2026